Progressive fracture of reinforced deck slab in girder-slab type bridge deck.

Muhammad Saleh. Al-Suwaiyan

Civil Engineering

07-12-1986

Abstract

An experimental investigation was conducted on two types of reinforced concrete deck slabs, restrained and unrestrained, to determine their static and fatigue life under a simulated wheel load. For the restrained panels, large size simulated girder-slab type bridge decks were cast and for the unrestrained panels, small size concrete slabs were used. One of the significant aspects of this study was to observe the influence of initial non-structural cracks in deck slabs which are caused by different phenomena such as plastic shrinkage, plastic settlement and thermal effects on the static capacity and fatigue of deck slabs. Two construction practices were followed, good and bad. The only difference between the two was in the curing method. Badly constructed panels were left to self cure in air immediately after casting in order to induce initial non-structural cracks, whereas well constructed panels were covered with polythene sheeting immediately after casting and water was sprayed twice a day for seven days. Static and fatigue tests were conducted on these panels using a 50T MTS actuator to apply a patch load that increased slowly until the failure was reached. The loaded area was kept small to induce punching type failure and to reflect the behavior under high abnormal loads exceeding the design limits. In fatigue tests a fraction of the ultimate static capacity was taken as the maximum load for the fatigue cycle, and the load ratio was kept close to 0. 1. Based on the test data, fatigue life has been prescribed in a nondimensionalized form which appears to be independent of the type of concrete.

Test results show that the static capacity of reinforced concrete deck slabs is impaired by the pressure of initial precracks and that it is enhanced to ascertain degree by edge restrained and increase in tension steel. Both static and fatigue failure under a highly concentrated patch load portray a localized punching type failure of a conical concrete whose top corresponds to the loaded area and bottom encompasses a relatively large area.

Progressive Fracture of Reinforced Deck Slab in Girder-Slab Type Bridge Deck

by

Muhammad Saled Al-Suwaiyan

A Thesis Presented to the

FACULTY OF THE COLLEGE OF GRADUATE STUDIES

KING FAHD UNIVERSITY OF PETROLEUM & MINERALS

DHAHRAN, SAUDI ARABIA

In Partial Fulfillment of the
Requirements for the Degree of

MASTER OF SCIENCE

In

CIVIL ENGINEERING

January, 1987

INFORMATION TO USERS

This manuscript has been reproduced from the microfilm master. UMI films the text directly from the original or copy submitted. Thus, some thesis and dissertation copies are in typewriter face, while others may be from any type of computer printer.

The quality of this reproduction is dependent upon the quality of the copy submitted. Broken or indistinct print, colored or poor quality illustrations and photographs, print bleedthrough, substandard margins, and improper alignment can adversely affect reproduction.

In the unlikely event that the author did not send UMI a complete manuscript and there are missing pages, these will be noted. Also, if unauthorized copyright material had to be removed, a note will indicate the deletion.

Oversize materials (e.g., maps, drawings, charts) are reproduced by sectioning the original, beginning at the upper left-hand corner and continuing from left to right in equal sections with small overlaps. Each original is also photographed in one exposure and is included in reduced form at the back of the book.

Photographs included in the original manuscript have been reproduced xerographically in this copy. Higher quality 6" x 9" black and white photographic prints are available for any photographs or illustrations appearing in this copy for an additional charge. Contact UMI directly to order.

UMI

A Bell & Howell Information Company
300 North Zeeb Road, Ann Arbor MI 48106-1346 USA
313/761-4700 800/521-0600

PROGRESSIVE FRACTURE OF REINFORCED DECK SLAB IN GIRDER-SLAB TYPE BRIDGE DECK

BY

MUHAMMAD SALEH AL-SUWAIYAN

A Thesis Presented to the
FACULTY OF THE COLLEGE OF GRADUATE STUDIES

UNIVERSITY OF PETROLEUM & MINERALS
DHAHRAN, SAUDI ARABIA

In Partial Fulfillment of the
Requirements for the Degree of

MASTER OF SCIENCE IN

CIVIL ENGINEERING

January, 1987

PRINTED BY: UPM PRINTING PRESS

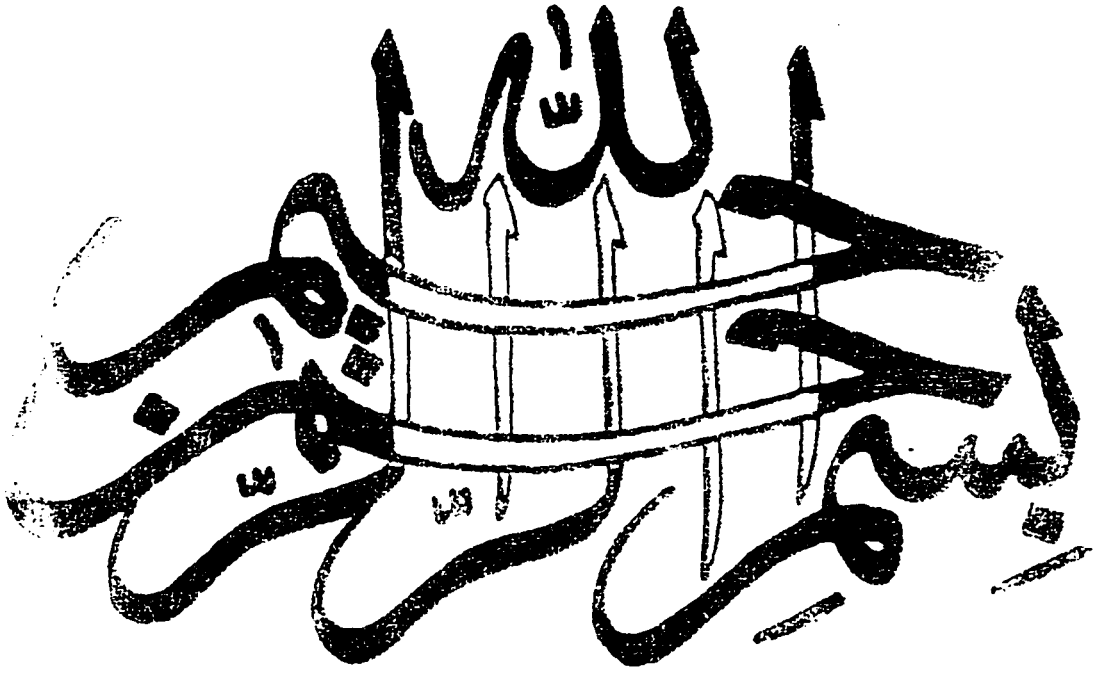
بسم الله الرحمن الرحيم

بسم الله الرحمن الرحيم

In the name of God, Most Gracious, Most Merciful

Say unto them, work as ye will;
but God will behold your work,
and his apostle also, and
the true believers.

SURAT. AL TAWBAH

Dedicated To

My Parents

UNIVERSITY OF PETROLEUM & MINERALS

DHAHRAN, SAUDI ARABIA

This thesis, written by

Muhammad Saleh Al-Suwaiyan

under the direction of his thesis committee, and approved by all the members, has been presented to and accepted by the Dean, College of Graduate Studies, in partial fulfillment of the requirements for the degree of

MASTER OF SCIENCE IN CIVIL ENGINEERING

Dr. Abdullah S. Al-Zakri
Dean, College of Graduate Studies

Date : Dec 7-86

Department Chairman

Thesis Committee

6.12.86
Chairman (Dr. A. K. Azad)

6.12.86
Co-Chairman (Dr. M. H. Baluch)

7-12-1986
Member (Dr. Mustafa Y. Al-Mandil)

ACKNOWLEDGEMENTS

The author wishes to thank the University of Petroleum and Minerals for its support throughout his study program.

The financial support for this work was provided by the National Project "A Study of Cracking of Concrete Bridge Decks in Saudi Arabia", founded by the King Abdulaziz City for Science and Technology (KACST). The writer gratefully acknowledges this support.

The author wishes to express his gratitude to his Committee Chairman and Major Advisor of the thesis Dr. A. K. Azad for his assistance and professional guidance throughout this work. The author also wishes to express his sincere appreciation to the Co-Chairman, Dr. M. H. Baluch, for his professional advice and invaluable suggestions. Thanks are also due to the Committee Member, Dr. M. Y. Al-Mandil, for his help and encouragement. Thanks are also extended to Dr. Alfarabi Sharif, Dr. Pearson-Kirk, Mr. Yasin Ziraba, Mr. Salahuddin Al-Sourti, Mr. Rolan, Mr. Omar Husain and Mr. Zaini, for their assistance in various aspects of this experimental work.

The author also records his appreciation to the Department of Civil Engineering for permitting to use the laboratory facilities.

Finally the author would like to thank Mr. Mumtaz Khan for typing the entire manuscript.

TABLE OF CONTENTS

List of Tables

List of Figures

List of Plates

الخلاصـــــة

أجريت اختبارات تجريبية على نوعين من البلاطات السطحية الخرسانيـــــة المسلحة ، مقيدة وغير مقيده ، لايجاد مقاومتها الاستاتية وحياتها الاكليلية عند تعريضها لحمل يحاكي الحمل القادم من عجلات العربات . بالنسبة للبلاطات المقيدة ، فقد صبت مجموعة من سطوح الجسور الكبيرة لتحاكي نوع عارضه سطوحه من سطوح الجسر . أما بالنسبة للبلاطات غير المقيدة فقد أستخدمت مجموعة من البلاطات الخرسانية البسيطة . أحد الأهداف المهمة لهذه الدراسة كان ملاحظة تأثير الثلوم الأولية الغير بنائية التي تظهر نتيجة لأسباب مثل : التقلص اللدن والترسب اللدن والتأثيرات الحرارية على المقاومة الاستاتية والحياة الأكيلية للبلاطات السطحية .

أتبعت طريقتان لبناء هذه البلاطات ، جيدة ورديئة . الفارق الوحيد بين هاتين الطريقتين كان في طريق الأنضاج . فبينما تركت البلاطات التي بنيت بالطريقة السيئة تنضج بنفسها في الهواء بمجرد صبها لكي تزداد فرصة تكون ثلوم أولية ، غطيت البلاطات التي أستعملت الطريقة الجيدة لبنائها بأغطية من البلوثين بمجرد صبها كما تم رشها بالماء مرتين يوميا لمدة سبعة أيام . أجريت الاختبارات الاستاتية والأكليلية على هذه البلاطات من خلال مثقل قدرته ٥٠ طن . أستعمل هذا الجهاز لأعطاء حمل على مساحة معينة من البلاطة . تمت زيادة هذا الحمل ببطء حتى التصدع . أستعملت مساحة صغيرة للحمل على البلاطات للحصول على انهيار خرمي ولكي ينعكس سلوك البلاطات تحت تأثير حمل كبير جدا يزيد عن حمل التصميم . في الاختبارات الاكليلية أخذ جزء من المقاومة الاستاتية كالحد الأعلى للدورة الأكليلية ، كما أستعملت نسبة حمل تساوي ار٠ . بناء على نتائج الاختبارات ، وصفت الحياة الاكليلية للبلاطات بواسطة أشكال غير بعدية بدت غير معتمدة على نوعية الخرسانة .

بينت الاختبارات أن المقاومة الأستاتية للبلاطات السطحية الخرسانيـــــة المسلحة تقل عند وجود ثلوم أولية غير بنائية وأنها تزداد لدرجة ما بسبب تقييد أطراقها أو بسبب زيادة التسليح . ان الانهيار الاستاتي والاكليلي بسبب حمل مركز على مساحة صغيرة يأخذ شكل خرم محلي من الخرسانة له شكل مخروطي يماثل سطحه العلوي شكل المساحة المعرضة للحمل بينما يمتد سطحه السفلي الى مساحة أكبر نسبيا .

ABSTRACT

An experimental investigation was conducted on two types of reinforced concrete deck slabs, restrained and unrestrained, to determine their static and fatigue life under a simulated wheel load. For the restrained panels, large size simulated girder-slab type bridge decks were cast and for the unrestrained panels, small size concrete slabs were used. One of the significant aspects of this study was to observe the influence of initial non-structural cracks in dech slabs which are caused by different phenomena such as plastic shrinkage, plastic settlement and thermal effects on the static capacity and fatigue life of deck slabs. Two construction practices were followed, good and bad. The only difference between the two was in the curing method. Badly constructed panels were left to self cure in air immediately after casting in order to induce initial non-structural cracks, whereas well constructed panels were covered with polythene sheeting immediately after casting and water was sprayed twice a day for seven days. Static and fatigue tests were conducted on these panels using a 50T MTS actuator to apply a patch load that increased slowly until the failure was reached. The loaded area was kept small to induce punching type failure and to reflect the behavior under high abnormal loads exceeding the design limits. In

fatigue tests, a fraction of the ultimate static capacity was taken as the maximum load for the fatigue cycle, and the load ratio was kept close to 0.1. Based on the test data, fatigue life has been prescribed in a nondimensionalized form which appears to be independent of the type of concrete.

Test results show that the static capacity of reinforced concrete deck slabs is impaired by the presence of initial precracks and that it is enhanced to ascertain degree by edge restraint and increase in tension steel. Both static and fatigue failure under a highly concentrated patch load portray a localized punching type failure of a conical concrete whose top corresponds to the loaded area and bottom encompasses a relatively large area.

CHAPTER 1

INTRODUCTION

1.1 General

Failure of structures subjected to cyclic loading at low values of stress was first observed in the mid eighteen century and is known since then as fatigue failure. Since this phenomenon was first observed in metal structures, much of the earlier research was limited to fatigue of metals. The fatigue life of a structure is often referred to the number of cycles it can sustain under a prescribed load or stress cycles. There are several factors that adversely influence the fatigue life of a structure. Two significant factors are the value of the maximum applied stress and the stress ratio of the load cycle. The stress ratio, R, is the ratio of the minimum to the maximum stress, a value of R = 1.0 represents the static case whereas R = -1.0 represents the complete reversal of stress which is the most critical condition for fatigue. It is well known that as the stress ratio decreases for a constant value of the maximum stress the fatigue life also decreases, whereas it increases as the

maximum stress is decreased for a constant stress ratio.

The plot of maximum stress, S, for a certain stress ratio versus the number of cycles to cause failure, N, known as S-N diagram is the curve that shows the fatigue life under different loads. It can be constructed by performing the fatigue life tests under different values of load and then using the data points to plot the relationship between the load (stress) versus number of cycles to failure. As the load (stress) is reduced the fatigue life increases. At a certain value of the load the fatigue is virtually independent of the applied load and this value of load (stress) is referred to as the endurance limit. A member subjected to repeated stress fluctuations below this endurance limit is unlikely to fail.

Bridge deck slabs are typical structural elements that are subjected to repeated loading from the traffic. In recent years, many bridge decks in the Kingdom of Saudi Arabia have suffered premature failure by developing localized pot holes by complete fracturing of the concrete slab. The major cause of this type of failure, often referred to as punching shear, appears to be the high level of truck loading, far exceeding the normal 'legal' limit. Such heavy truck loads which were rampant at one time when no controls were existed, caused considerable damage to the bridges in the Kingdom. It is of interest to study the

failure of a deck slab under repetitive wheel loads which are much higher than the design load to objectively determine the fatigue life and observe failure pattern.

1.2 Literature Review

It has been reported that a bridge deck slab supported by a set of longitudinal beams and transverse diaphragms designed according to the conventional design will have much higher load carrying capacity than the ultimate load predicted by the common flexure theory (1). This increased capacity is attributed to the favorable lateral support restraints provided by the beams and diaphragms which develop in-place compressive forces and end moments in the slab. These forces and moments result in compressive stresses in the slab which enhance its load carrying capacity (2).

Tests and analytical studies of laterally restrained reinforced concrete slabs subjected to concentrated loads have been reported by Taylor (3), Aoki and Seiki (4), Bachelor (5, 6) and others. These studies have shown that compressive membrane stresses created by the lateral restraint at the slab boundaries as the slab deflects will increase the ultimate concentrated load when failure occurs in flexural mode, i.e. with the formation of a yield line pattern. Lateral restraint has also been found to result in

an increase in the ultimate concentrated load when failure occurs in a shear mode due to punching.

In 1960 Kinnunen and Nylander (7) studied the punching of simply supported reinforced concrete slabs. First they performed many static tests on circular concrete slabs without shear reinforcement and then they developed a model that allows one to calculate the ultimate strength of slabs without shear reinforcement. In reference (8) Kinnunen extended the above slabs with two-way reinforcement. In 1965 Taylor and Hays (3) reported some test results on the effect of edge restraint on punching shear capacity of reinforced concrete slabs. The tested slabs were 2 ft. 11 in. square and 3 in. deep and the edge restraint was provided by a steel frame surrounding the slab. The main conclusion of this work was that the enhancement of the load carrying capacity due to the restraint is higher for slabs having low reinforcement ratios.

Many researches (4, 9, 10) have shown that restraining the edges of the slab against movement can enhance its punching strength. However, no universal approach for the design of restrained slabs have been developed and empirical approaches to this problem have been found more fruitful. In 1975, Hewitt and Batchelor (2) described a recent investigation of a rational approach for calculating the punching strength of restrained slabs. A model of punching

failure was developed for calculating the punching load of a slab with known boundary restraints. An empirical factor, which can be deduced from tests, was proposed for use in prediction of the punching strength of slabs whose boundary restraints are not exactly known.

In 1958, a review (11) of research on fatigue of concrete revealed a sparsity of knowledge of the fatigue of concrete slabs. Since then, although many fatigue studies have been conducted on plain concrete and reinforced concrete beams, very little attention has been given to the punching type failure of deck slabs under repeated loadings. In (12) Ralejs and Kutti proposed an equation for the determination of the fatigue strength of plain, ordinary and light weight concrete when subjected to compressive stresses. The proposed equation can be used to plot S-N curves for constant stress ratios. This equation was verified by laboratory experiments carried by the authors and by data taken from the literature. In 1979, Ralejs extended the equation to tensile fatigue strength of plain concrete.

Many references (13, 14, 15, 16, 17, 18) studied the fatigue of reinforced concrete, mainly reinforced concrete beams. In reinforced concrete the fatigue strength of the structure will be governed either by the fatigue life of the concrete or by the fatigue life of the reinforcement. When

the static shear and flexural strength of a concrete beam are approximately equal this beam can fail by fatigue of the reinforcement or in shear by either a diagonal cracking failure or shear compressive failure (18). Week in Ref. (19), discussed the fatigue strength of reinforcing bars in concrete beams.

In 1975,, Bachelor and Hewitt (20) did some tests on five 1/8 scale direct models of an 80 ft. single span four-beam composite steel/concrete bridge. Most of the panels failed by punching in a sudden and explosive manner when tested to failure under fatigue loading.

Limited fatigue tests on small scale models have also demonstrated that the maximum load under the fatigue cycle to cause failure in number of cycles exceeding one million was also greater than the design loads (1). The limitations of this study were that the carefully constructed model sizes were too small to ideally represent the in-situ deck slab and that no attempt was made to study the effect of initial pre-cracks (non-structural) that are invariably present due to various environmental and construction related causes.

Limited research has been conducted on the fatigue life of reinforced concrete slabs under the action of concentrated loads. Okada, Okamura and Sonoda (21) investigated the behavior of concrete slabs under repetitive

loading. Their aim was to clarify the fatigue mechanism of reinforced concrete slabs under moving loads. Seven slabs with full scale dimensions were tested under static and cyclic loads. To investigate deflection characteristics and reserve fatigue strength of cracked slabs subjected to actual traffic loads, especially, four test slabs were sawn out from two distressed bridge decks. Experimental findings were mainly as follows: rubbing together of crack faces due to the repeatedly moving loads eventually produced a slit with a narrow opening in the cracked section; the formation of the slit reduced both flexural and shearing rigidities of the slab; if rain water was poured into the cracked section, the reduction of these rigidities was remarkably accelerated and caused the slab surface to collapse prematurely (21, 22).

1.3 Scope and Objectives

A review of the past work on the study of fatigue failure of deck slabs under cyclic load shows that limited work has been carried out so far. Past studies have not considered the influence of numerous pre-cracks that normally exist in a slab due to various causes attributed to plastic shrinkage, plastic settlement and thermal effect on the progressive fracture under cyclic load. Furthermore it is also necessary to determine the fatigue life at high

stress level to demonstrate the damaging effect of such high loads which may cause premature punching failure. In order that test data would be meaningful and not significantly influenced by the size effect, the experimental work needs to be carried out on relatively large size simulated bridge decks. The broad objectives of this work are as follows:

1) Study the behavior of reinforced concrete slabs under a repetitive concentrated load and determine their fatigue life corresponding to various maximum stress levels.
2) Study the influence of the edge restraint provided by the longitudinal beams and transverse diaphragms on the static load carrying capacity and fatigue life of the slab by comparing both these values for restrained and unrestrained slabs.
3) Study the adverse influence, if any, of the initial non-structural cracks that exist in the slab due to various causes such as plastic shrinkage, plastic settlement and thermal effect on the static capacity and the fatigue life of reinforced concrete slabs.
4) Observe the effect of the amount of the steel reinforcement on the mode of failure and the capacity of the slab.

A test program was engineered in which thirteen simulated deck panels and sixteen simple slabs were tested

to derive test data. From static tests, the ultimate load carrying capacity, Pu, under a patch load (simulating the action of a wheel load) was determined. The area of the patch load was kept small to ensure punching type failure. Using various fractions of the ultimate load, ranging from 0.60 Pu to 0.90 Pu, fatigue tests were conducted to find the fatigue life and plot S-N diagrams. A significant aspect of this study was to examine the adverse effect of non-structural pre-cracks in the punching type failure.

CHAPTER 2

EXPERIMENTAL PROGRAM

The program mainly consisted of casting two types of deck slabs, restrained and unrestrained slabs and testing them to evaluate their load carrying capacity under both static and cyclic loads. For both types of test panels, the significance of good and bad construction was observed. The basic difference between good and bad construction was in the method of curing. The bad construction practice was meant to initiate non-structural pre-cracks. This chapter describes comprehensively the details of the test program.

2.1 Test Specimens

2.1.1 *Unrestrained Panels*

A total of sixteen panels, eight following bad construction practice and the remaining eight following good construction practice were cast. The panel size was 38 cm x 79 cm x 7.6 cm and the typical reinforcement arrangement is shown in Fig. (2.1). Two different values for the tensile reinforcement were used as shown in Table 2.1. The mix design that was used for these panels is as follows: Coarse

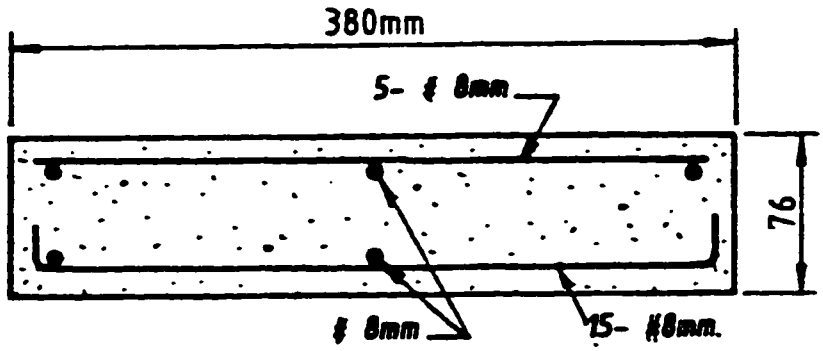

(a) UGL & UBL Series

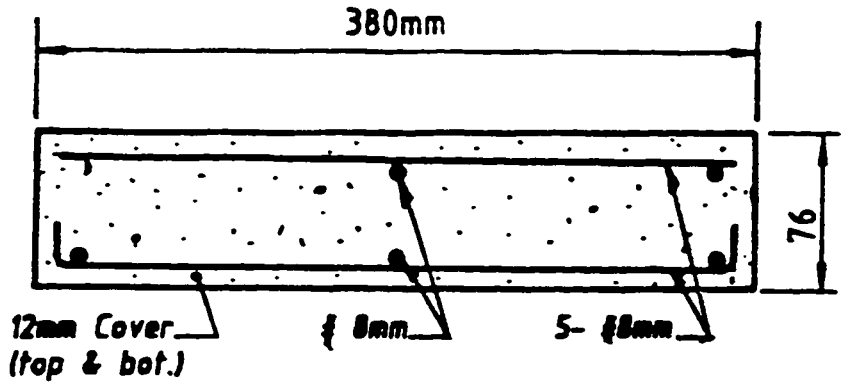

(b) UGH & UGH Series

Fig. 2.1: Details of Unrestrained Panels.

Table 2.1: Unrestrained Panels Designations

PANEL TYPE	CONSTRUCTION	DETAILS OF TENSILE REINFORCEMENT
UGH1 to UGH4	Good	15 - # 8mm bars
UBH1 to UBH4	Bad	15 - # 8mm bars
UGL1 to UGL4	Good	5 - # 8mm bars
UBL1 to UBL4	Bad	5 - # 8mm bars

aggregate to fine aggregate ratio = 2.21, total aggregate to cement = 5.4, water-cement ratio w/c = 0.75 and cement content = 360 kg/m^3. The maximum size of coarse aggregate used was 12mm (1/2 in.). The aggregates used were unwashed and had an absorption of about 5%, reflecting a higher demand of water-cement ratio for a workable mix.

The bad construction practice as defined in this work was related to casting in outdoor windy conditions with an average temperature of 36^{o}C and relative humidity of 40%. In the absence of wind, the windy conditions were simulated by blowing air from electric fans. The panels were left outside for self curing with no moisture supplement. This practice would give rise to uncontrolled random non-structural pre-crack related to plastic shrinkage, plastic settlement and drying shrinkage.

On the other hand, good construction was achieved by casting the panels inside the laboratory (average temperature 30°C and relative humidity 30% and no wind) followed by water sprayed twice a day for seven days. The good panels were covered by polythene sheeting immediately after casting and trowel finishing to prevent rapid loss of moisture from the top surface.

Two different amounts of bottom (tension) steel in the short direction were used to indicate if the failure mode in fatigue is influenced by the amount of tension steel.

Strain gages were attached to the tension reinforcement of three of these panels in order to examine the stress and the variation of stress in the rebars.

2.1.2 *Restrained Panels*

Due to limitations of testing and casting facilities, it was not possible to choose panel dimensions by directly scaling down a particular prototype deck. Instead, the dimensions of a typical panel as shown in Fig. 2.2 was selected for tests, representing a hypothetical girder-slab type bridge deck model. A typical panel consists of 100mm reinforced concrete slab supported by three steel I-beams of length 1.53 spaced at 710mm centers. The slab cantilevered on both sides by 190mm. To ensure composite action, 12mm diameter studs were welded to the top flange of the supporting beams. The lateral restraint provided by the supporting longitudinal beams play a vital role in the behavior of the deck slab. Though this restraint may induce unwanted shrinkage cracks in the slab due to restriction on the free lateral contraction, it favourably influences the load carrying capacity of the slab, the increased capacity being related to the degree of restraint.

While the geometry, distribution steel and the slab thickness were kept the same, both top and bottom steel had two different values. One set of panels had tension steel

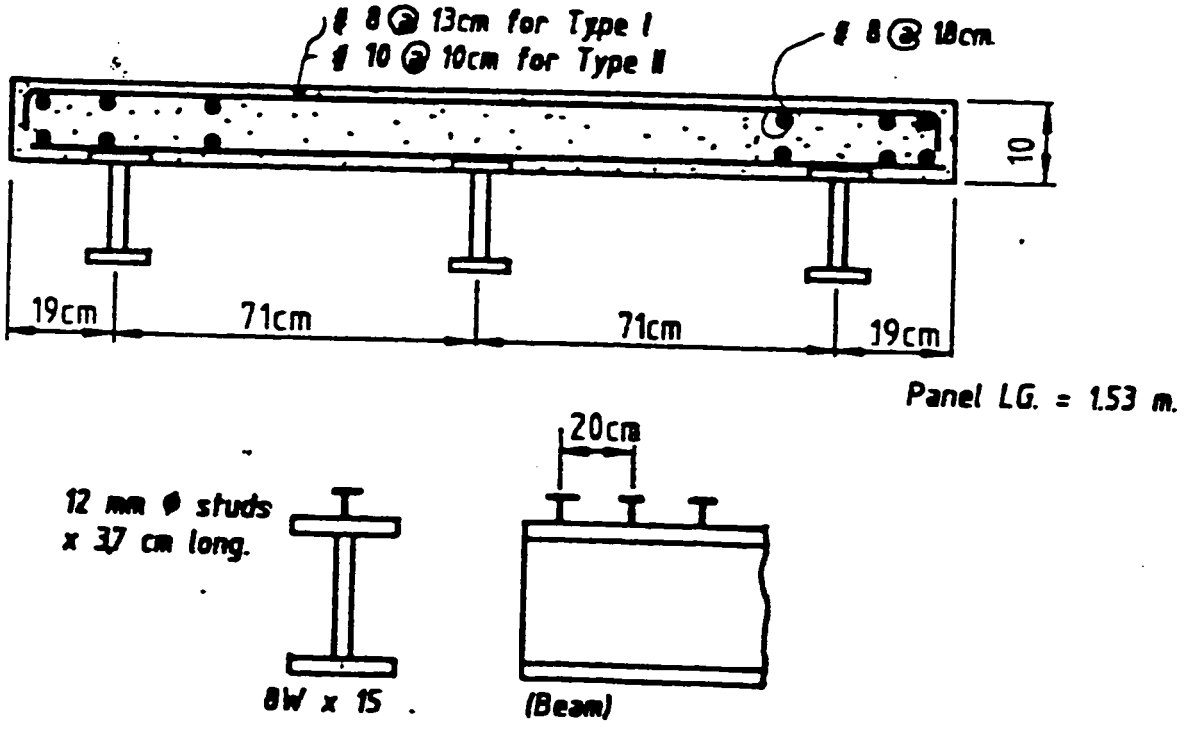

Fig. 2.2: Details of Restrained Panels.

ratio ρ = 0.0048, and the other set had a higher amount of steel corresponding to ρ = 0.0092.

All restrained panels were cast using good and bad construction practice. The only difference between the two here was the method of curing, as all panels were cast in outdoor environment using the same concrete mix. The good panels immediately after casting were covered with polythene sheets and cured with water sprayed twice a day for seven days. The bad panels were left uncovered to permit rapid evaporation of moisture and were allowed to self cure in air without moisture supplement. In addition, windy environmental conditions were simulated for bad panels by blowing fans in order to induce plastic shrinkage cracks. Plates 2.1a through 2.1d show the non-structural precracks in the bad restrained panels.

The concrete for this large scale pouring was supplied by a local ready-mix contractor in accordance with the following specified mix design: Coarse aggregate to fine aggregate ratio = 2.0, total aggregate to cement = 5.5, water-cement ratio w/c = 0.57 and cement content = 370 kg/m^3. The maximum size of coarse aggregate was 12mm (1/2 in.). The aggregate used was washed and had a water absorption of 1.7%. In addition to the panels, 75 x 150mm cylinders were cast to obtain data on the 28-day compressive strength.

A total of thirteen panels were cast in two sets. One

Plate 2.1a: Non-Structural Cracks in Restrained Panels.

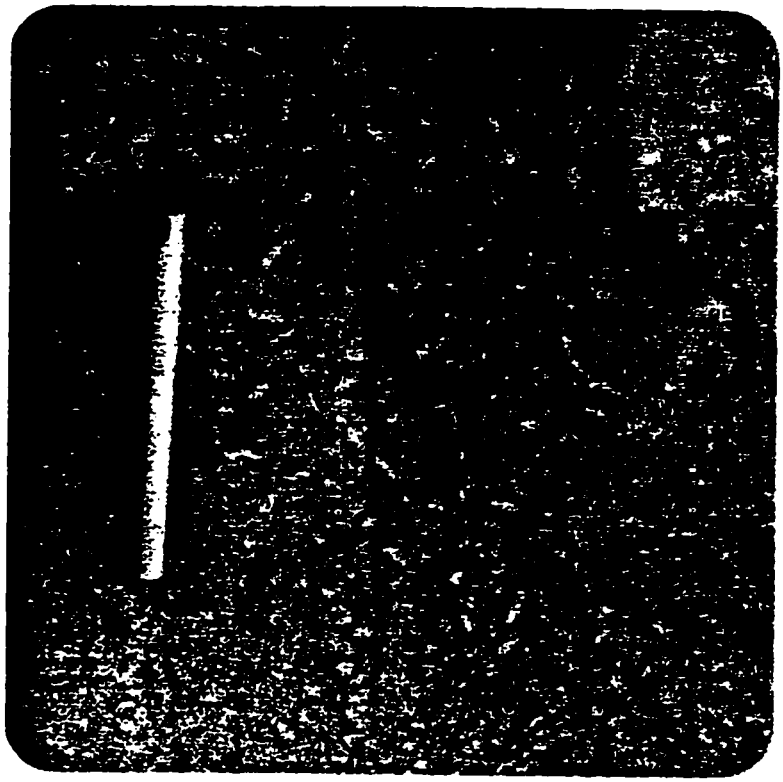

Plate 2.1b: Non-Structural Cracks in Restrained Panels.

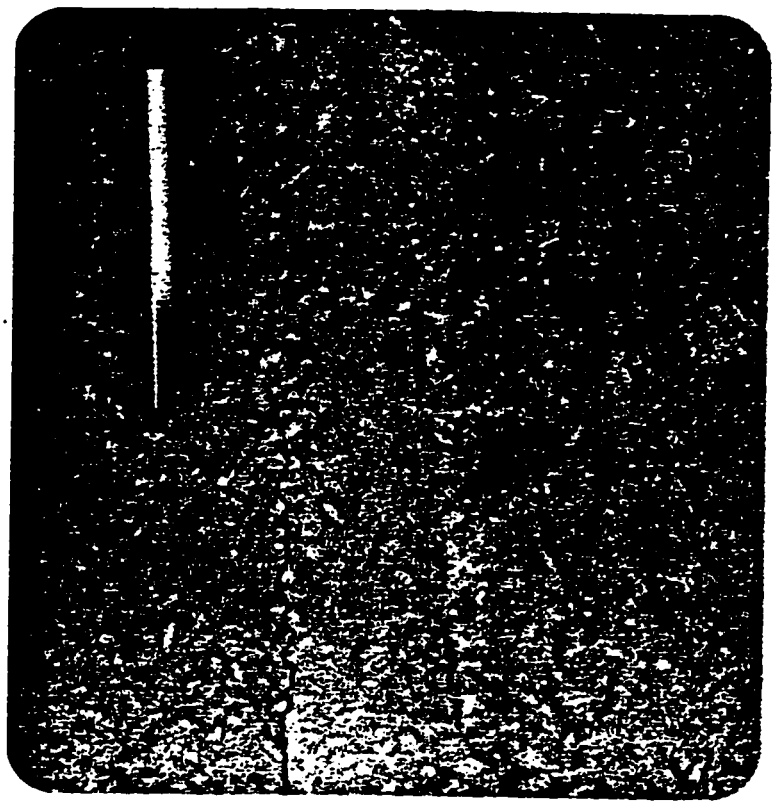

Plate 2.1c: Non-Structural Cracks in Restrained Panels.

Plate 2.1d: Non-Structural Cracks in Restrained Panels.

Table 2.2: Restrained Panels Designations

PANEL DESCRIPTION	No. of Panels	PANEL DESIGNATION	Percentage Steel
Bad construction, low steel	4	RBL1 to RBL4	0.48
Good construction, low steel	4	RGL1 to RGL4	0.48
Good construction, high steel	5	RGH1 to RGH5	0.92

set of good and bad panels were cast with low tension steel (ρ = 0.48%) and another set of good panels were cast with heavy tension steel (ρ = 0.92%). The same amount of tension steel was used both at top and bottom of the slab as shown in Fig. 2.2. The distribution steel in the longitudinal direction was kept unchanged for all panels. Table 2.2 lists the three types of restrained panels and their designations.

2.2 Test Set-up and Procedure

Testing of all panels was conducted under a test frame with a 50T MTS actuator as shown in Plate 2.2. For some panels the deflection was measured using LVDT, and for those panels fitted with strain gages, strains were also recorded.

2.2.1 *Testing Procedure for Restrained Panels*:

The deck panel was supported by two large steel beams to provide a simple span of 1.3m. A single patch load was applied to the mid span of the deck slab by pressing the actuator's head onto a rubber padded steel plate, Fig. 2.3.

For static tests, the load P in Fig. 2.3, was slowly increased until the slab failed. The crack pattern at the bottom of the slab was observed continuously. Two values of the loaded area were used for the static test, 50 x 100mm and 100 x 200mm. For two panels the deflection of the slab

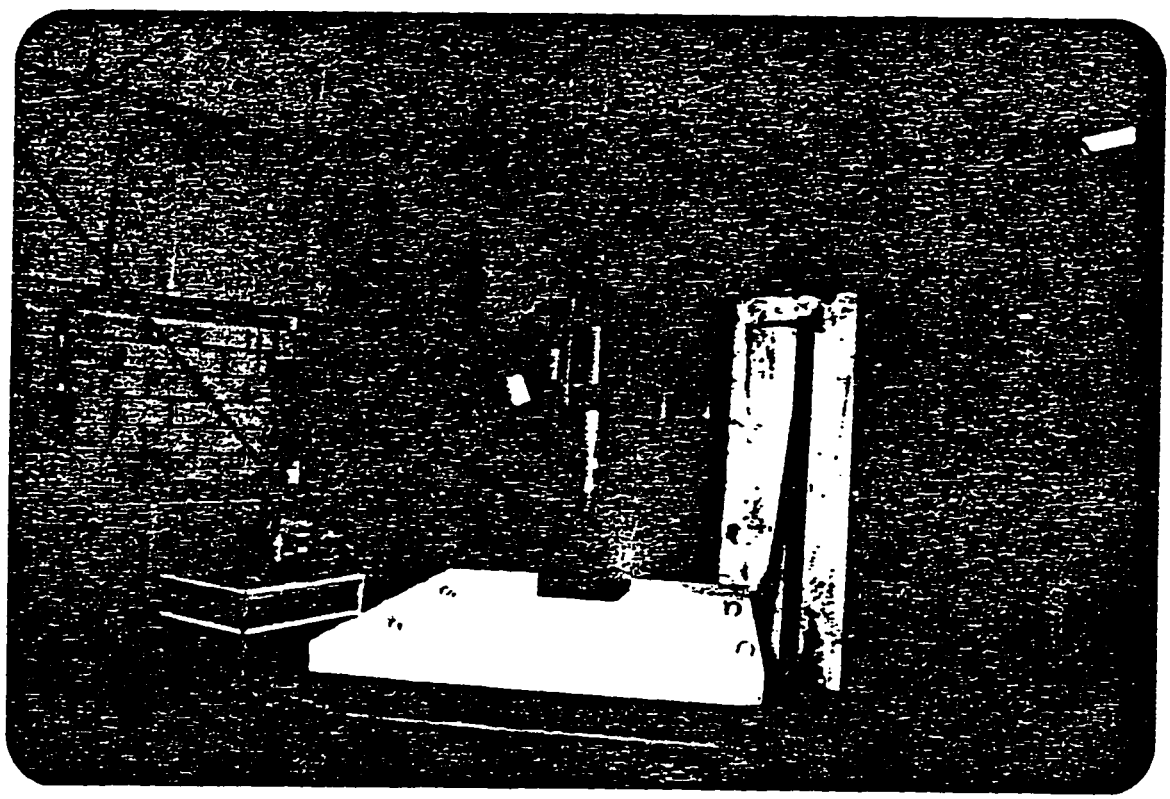

Plate 2.2: Test Set-up for Restrained Panels.

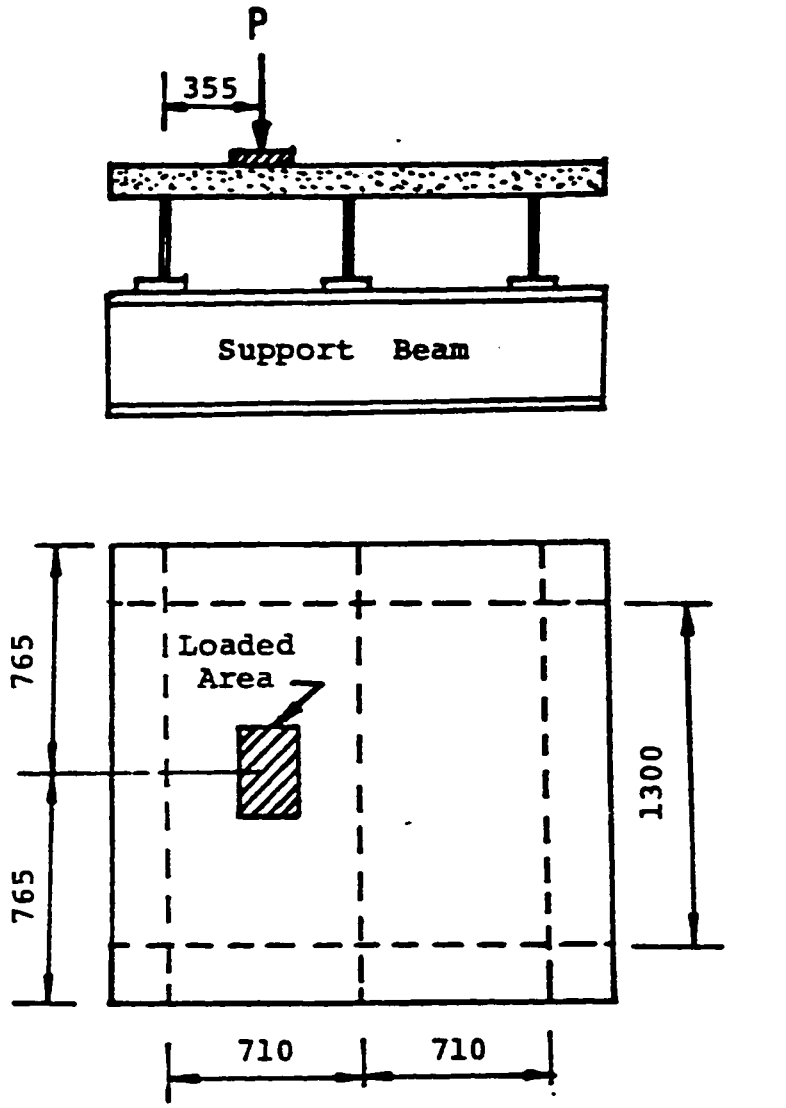

(All dimensions in mm.)

Fig. 2.3: Loading of Restrained Panels

under the point of application of load and the midspan of the supporting beams was monitored using LVDT to obtain the load deflection response of the deck slab.

For fatigue tests, the maximum load was selected corresponding to a chosen fraction of the static ultimate capacity of the slab. The load was cycled between this maximum value and a small residual value to yield a load ratio R = 0.1. The value of R was kept constant for all fatigue tests. The maximum load was restricted to four different values corresponding to 0.9 Pu. 0.8 Pu, 0.7 Pu and 0.6 Pu, Pu being the ultimate failure load as determined from the static tests. The frequency of the load cycles was in the neighbourhood of 2 Hz for all fatigue tests. The loaded area was restricted to 50 x 100mm for all fatigue tests.

As the failure of the deck slab under a single patch load was essentially localized, it was possible to utilize both slab spans of a panel to derive two test data from each panel.

2.2.2 *Testing Procedure for Unrestrained Panels*:

The deck slab was supported along the long edges by two I-beams to provide a simple span of 340mm. A 12mm diameter rod was welded to the top flange of the steel beam and a plate of 12mm width with a groove was placed on top of the

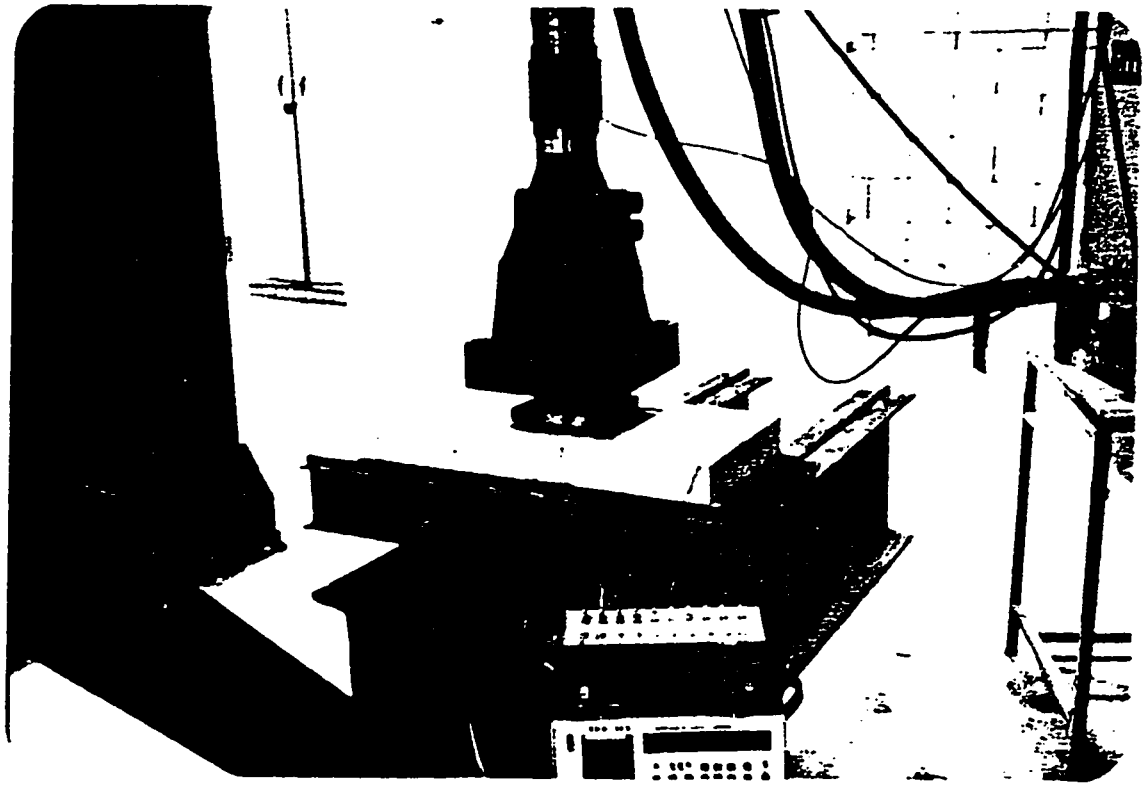

Plate 2.3: Test Set-up for Unrestrained Panels.

bar to permit rotation of the edges of the slab. A typical set up is shown in Plate 2.3.

For static tests, the load was applied to the center of the panel by the actuator's head pressing slowly onto a 32 x 64mm rubber padded steel plate until the panel failed. For three panels the strains in the tension reinforcement were monitored using a strain gage reader. For the fatigue tests the same procedure used for restrained panels was followed.

CHAPTER 3

COMPUTATION OF FAILURE LOADS

In this chapter, an attempt has been made to compute theoretical values of failure loads of the deck slabs under a single patch load considering both the flexural and the punching failure. For the former case, the yield line theory which is considered to be more appropriate for slabs has been used. For calculation of punching capacity, two methods which have been advocated to be more exact have been used.

3.1 Flexural Capacity

3.1.1 *Introduction to Yield Line Theory*:

The method for the limit analysis of reinforced concrete slabs known as yield line theory was initiated by Ingerslev (26) and greatly extended and advanced by Johansen (27). This method is an upper bound approach. The ultimate load of a slab is estimated by postulating a collapse mechanism which is compatible with the boundary conditions. The moments at the plastic hinge lines are the ultimate moments of resistance of the sections, and the ultimate load is determined using the principle of virtual work or the

equations of equilibrium. Being an upper bound approach the method gives an ultimate load which is correct only when the assumed collapse mechanism corresponds to the correct one, otherwise the method yields an overestimated ultimate load.

The fundamental assumptions that are made in order to apply this method to the ultimate load analysis are:

1) The collapse mode is a flexural one, that is, that the slab has sufficient shear strength to prevent a premature shear failure.
2) The reinforcing steel is fully yielded along the yield lines at failure.
3) The slab deforms plastically at failure and is separated into segments by the yield lines.
4) The elastic deformations are negligible compared to the plastic deformation, i.e. the slab parts rotate as plane segments in the collapse condition.
5) The bending and twisting moments are uniformly distributed along the yield line and they are the maximum values provided by the ultimate moment capacities in two orthogonal directions.

The correct collapse mechanisms in nearly all common cases are well known and therefore one is not often faced with the uncertainty of whether further alternatives exist.

3.1.2 *Analysis of Deck Slabs*:

A restrained panel can be analysed using yield line theory by considering it as a continuous two-way slab. The virtual work method can be employed to determine the collapse load.

To analyse a slab by the virtual work method, a yield line pattern is postulated for the slab at the ultimate load. The segment of the yield line pattern may be regarded as rigid bodies because the slab deformation with further deflection occurs only at the yield lines. The segments of the slab are in equilibrium under the external loading and the internal forces along the yield lines. A convenient point within the slab is given a small virtual displacement in the direction of the load, then the resulting displacements at all points of the slab, δ (x, y), and the rotations of the slab segments about the yield lines may be found in terms of δ and the dimensions of the slab segments. Work will be done by the external loads and by the internal actions along the yield lines. When the virtual work equation is applied to a particular slab the displacement term cancels from the equation and the ultimate load is given in terms of the slab dimensions and the ultimate moments of resistance per unit width. In Fig. 3.1a the assumed failure mechanism (yield line pattern) for the slab

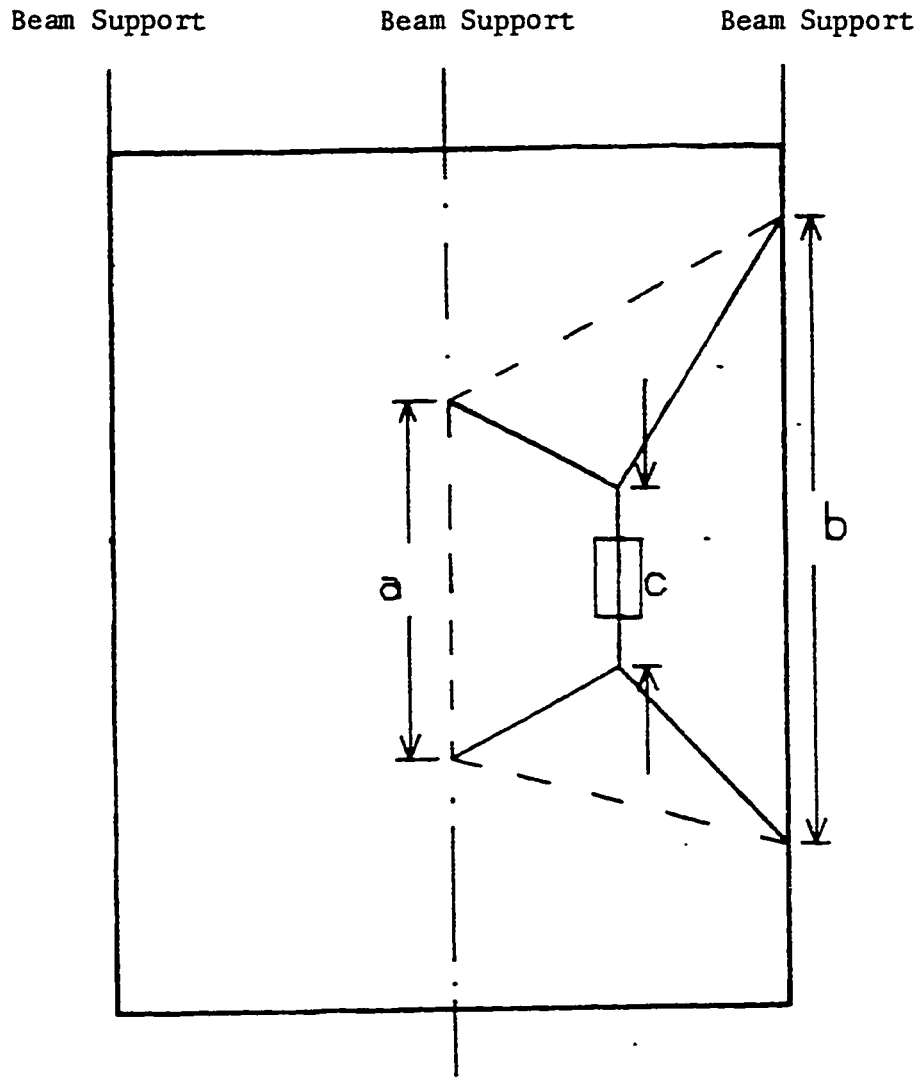

Fig. 3.1a: Yield Line Pattern for Restrained Slabs.

under consideration is shown. This pattern which is considered to be the most appropriate depends on three variables a, b, c. The length of the yield lines a, b and c must be determined to produce minimum value of Pu. The yield line analysis gives the ultimate capacity of the slab as:

$$Pu = 2\frac{Mu}{L}\{2a + b + \frac{b - a}{a - 2c + b}(2b - c - a)\} + 16\frac{M_t L}{a - 2c + b} \quad \text{.....(3.1)}$$

Using a computer program, minimum value of Pu was determined by a search procedure in which the three variables a, b and c were progressively varied, one at a time.

It was found that the ultimate capacity of the panels is a linear function of the dimension c, i.e. the smallest capacity corresponds to the minimum value of c. The minimum feasible value that c can take must be the width of the bearing plate which is in this test was confined to 100 mm (4 in.) and 200 mm (8 in.).

The values of Pu computed in this manner are shown in Table 3.1 for the panels of high and low steel along with the values of yield lines dimensions a, b and c. Results are shown for both loaded areas of 50 x 100 mm (2 x 4 in.)

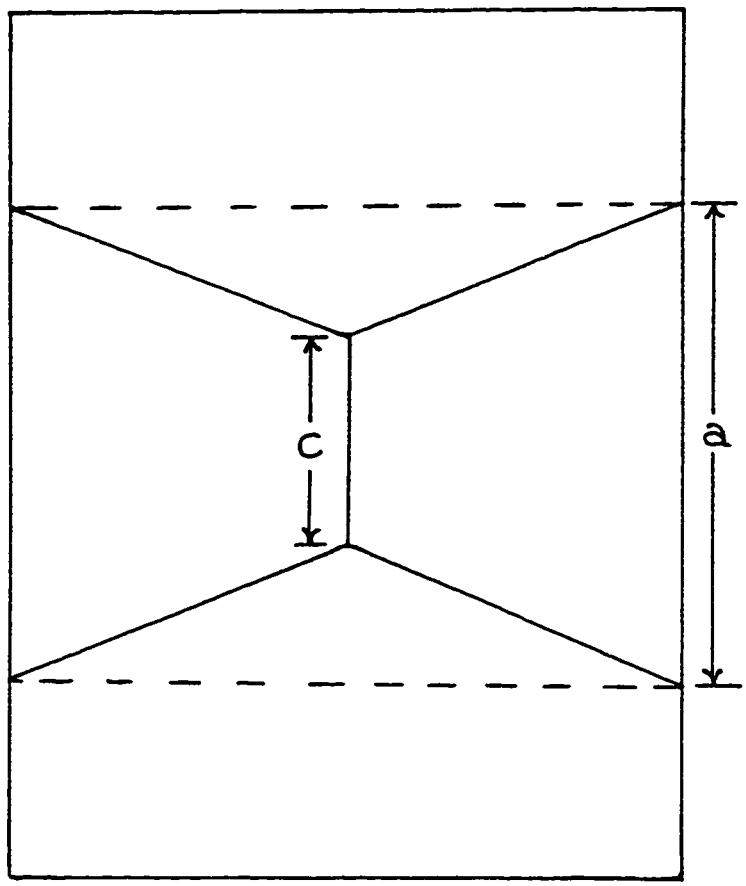

Fig. 3.1b: Yield Line Pattern for Unrestrained Slabs.

Table 3.1: Ultimate Flexural Capacity of Restrained Slabs

Panel Type	Bearing Area	a (in)	b (in)	c (in)	Ultimate Capacity (kN)
High steel $\rho = 0.0092$	100 x 200 mm	27	27	8	210
	50 x 100 mm	23	23	4	195
Low Steel $\rho = 0.0048$	100 x 200 mm	33	33	8	148
	50 x 100 mm	29	29	4	138

Table 3.2: Ultimate Flexural Capacity of Unrestrained Slabs

Panel Type	Bearing Area	Capacity (kN)
High steel $\rho = .0173$	32 x 64 mm	110
Low steel $\rho = .0056$	32 x 64 mm	60

and 100 x 200 mm (4 x 8 in.). Since small variation in concrete strength does not appreciably alter the value of the ultimate moment of resistance for underreinforced section (which is the present case), the value of the ultimate loads in accordance with the yield line theory are essentially the same for panels of both good and bad construction.

Similarly the flexural capacity of unrestrained panels can be calculated. Table 3.2 gives the ultimate capacity of the unrestrained panels.

3.2 Punching Capacity

The punching capacity of the reinforced concrete deck slabs considered in this study are evaluated using two approaches to verify the applicability of these methods. The first one was developed by Kinnunen and Nylander (7) and the second approach is based on the theory of plasticity (24) Both approaches do not take into account the effect of the edge restraint in calculating the punching capacity of the slab. By comparing the experimental values with these values the effect of edge restraint is observed.

3.2.1 *Evaluation of Punching Capacity Using Kinnunen and Nylander Model*:

Based on experimental observations and findings,

Kinnunen and Nylander proposed an indealized model for a slab at punching failure. The outer portion of the slab, which is bounded by the shear crack and the radial cracks, is considered loaded through a compressed conical shell that develops from the loaded area to the end of the shear crack. This shell is assumed to have the shape indicated in Fig. 3.2.a, and its thickness is assumed to vary in such a manner that the compressive stresses at the intersection with the loaded area and at the root of the shear crack are approximately equal. The element in Fig. 3.2b is acted on by five forces which are: (i) the external load or reaction, (ii) the oblique compression force in the compressed conical shell, (iii) horizontal forces in the circumferential reinforcement at right angles to the radial cracks, R_3 , (iv) horizontal forces in the radial reinforcement traversing the shear crack, R_2 and (v) horizontal tangential compressive forces in the concrete, R_1.

Failure is described as the failure of the conical shell in compression which takes place when the tangential strain reaches a characteristic tangential value. Kinnunen and Nylander established relationship between the characteristic tangential strain and the slab loaded area dimensions, and between the tangential stress and the stress in the conical shell, which yielded agreement between the experimental and theoretical results. An increase of 20%

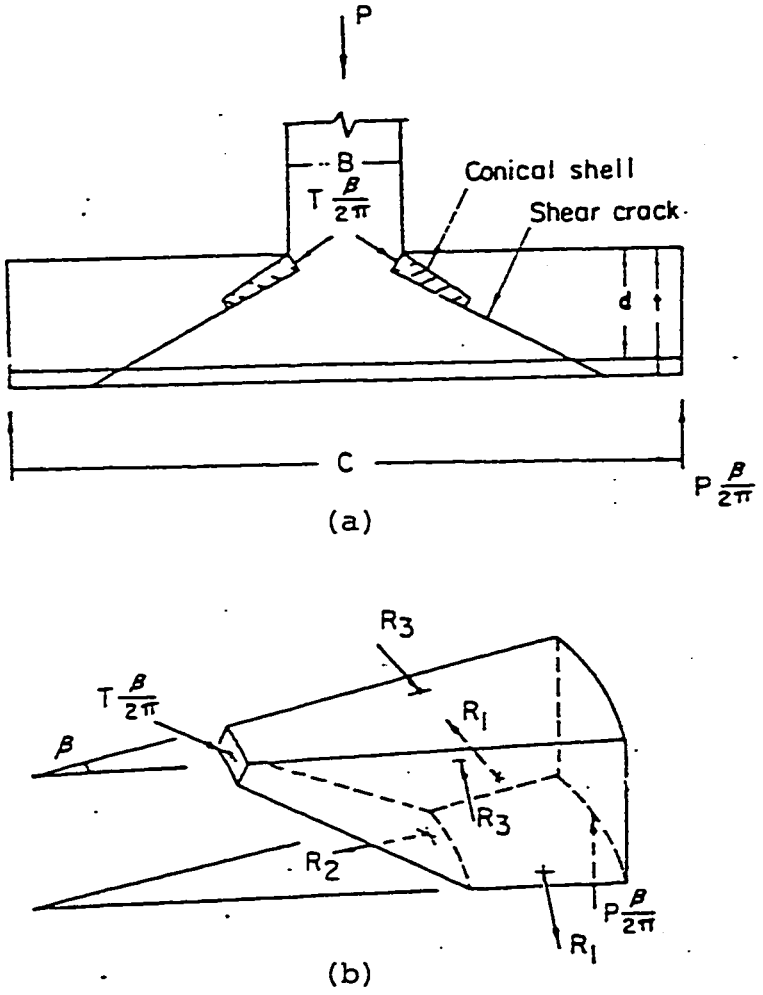

Fig. 3.2: Kinnunen and Nylander Model

Table 3.3: Punching Capacity of Restrained Panels Based on Kinnunen and Nylander Model

Panel Type	Loaded Area	Punching Capacity (kN)
BL	50 x 100 mm	72
	100 x 200 mm	88
GL	50 x 100 mm	70
	100 x 200 mm	82
GH	50 x 100 mm	100
	100 x 200 mm	109

for dowel action provided by the reinforcing was suggested by Hewitt and Bachelor in Ref. (2). The theoretical development of this model is given in Ref. (7).

A computer program was developed which calculates the punching capacity using this model. The input for this program are: slab and loaded area dimensions, reinforcement ratio and properties of the materials. This program is given in the Appendix.

Table 3.3 gives the theoretical capacity of the restrained slabs considered in this study using this model.

This method failed to give the capacity for small panels which implies that there are limitations for the use of this method.

3.2.2 *Evaluation of Punching Capacity Using the Theory of Plasticity*:

The failure mechanism considered here is the punching out of a solid of revolution, while the rest of the slab remains rigid as shown shown in Fig. 3.3. The effect of reinforcement is neglected in the development of this approach.

An upper bound ultimate punching load is found by equating the work done by the external load to the energy dissipated in the failure surface. The shape of the failure surface that corresponds to the lowest upper bound is determined using calculs of variation. The theoretical

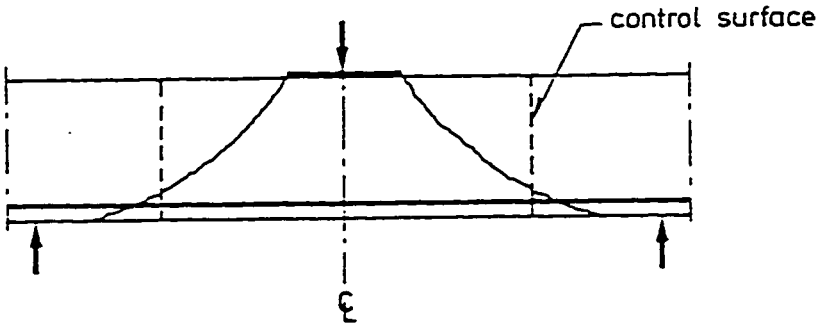

Fig. 3.3: Failure Mode considered in Plasticity Approach.

Table 3.4: Punching Capacity of Restrained Panels Based on Plasticity Approach.

Panel Type	Loaded Area	Punching Capacity (kN)
BL	50 x 100 mm	78
	100 x 200 mm	110
GL	50 x 100 mm	70
	100 x 200 mm	78
GH	50 x 100 mm	70
	100 x 200 mm	102

Table 3.5: Punching Capacity of Unrestrained Panels Based on Plasticity Approach

Panel	Punching Capacity (kN)
UBH1	39
UGH1	43
UBL1	37
UGL1	35

development for this approach is given in Ref. (24). Also, an iterative process is given to evaluate the punching capacity in addition to graphs that allow one to calculate the punching capacity of a slab as a function of its dimensions.

The main weakness of this model lies in the fact that its application is confined to the axisymmetric case and that it does not take the effect of steel reinforcement into consideration. However, this method was used to evaluate the punching capacity of both types of slabs considered in this study. Table 3.4 gives the punching capacity of restrained panels while Table 3.5 gives the punching capacity of unrestrained panels.

CHAPTER 4

TEST RESULTS AND DISCUSSION

Results of tests on reinforced concrete deck slabs are presented and discussed in this chapter. For clarity of presentation, restrained panels and unrestrained panels, are itemized separately.

4.1 Restrained Panels

The compression tests for the cylinders revealed that the compressive strength was significantly different for the two batch mixes used in casting. The main reason of this variation of strength could be attributed to the negligence of the readymix contractor in strictly adhering to the mix design specification. In view of this and the possibility that the actual concrete strength of each panel may vary due to variation in placement time and finishing, it was considered essential to extract cores from each panel to obtain a better estimate of the actual concrete strength. From each panel, two cores of 64mm (2 1/2 in.) diameter were drilled for testing. This diameter was the maximum that could be used to keep the height/diameter ratio not less than 1.5. For comparison purposes, the concrete strength

f'_c, as determined from these cores was used for the assessment of test data.

4.1.1 *Static Tests*:

The restrained panels were classified into three groups according to the amount of tension steel and curing conditions. These three types are: (i) bad construction with low steel (BL), (ii) good construction with low steel (GL) and (iii) good construction with heavy steel (GH). Two different loaded areas (bearing areas) were used to evaluate static load carrying capacity of the panels.

Table 4.1 shows the results of ultimate failure loads, Pu, in static tests along with the values of the core strengths and the ACI (25) punching load for a bearing area of 50 x 100mm (2 x 4 in.). Results indicate that the ultimate load carrying capacity of good panels with low steel was generally higher than that of badly constructed panels with low steel. A better comparison could be made by considering the average failure load and core strength and adjusting Pu values for the variation of the concrete strength from a reference strength by multiplying with a correction factor. This correction factor can be taken as a square root of the ratio of the core strengths, since the punching shear capacity is related to the square root of the concrete strength.

Table 4.1: Static Tests for Restrained Panels Using a Bearing Area of 50 x 100 mm.

Panel	Core Strength N/mm^2	Ultimate Failure Load Pu (KN)	ACI Punching Load (KN)
BL1/1	21.0	103	78
BL3/2	18.7	90	74
GL1/1	13.8	105	63
GL3/1	21.6	126	79
GH1/1	16.8	152	70
GH2/2	18.5	125	73

Introducing this correction factor, results of Table 4.1 are reproduced in Table 4.2 for an average core strength of each panel type. Results show that the load carrying capacity of panels of good construction increased by about 20%. It should be reiterated here that only difference between the good and bad panels was the method of curing. Compared to good panels, bad panels had more construction related initial cracks. The decreased load carrying capacity of the badly constructed panels is therefore solely attributable to the damaging effect of the non-structural cracks. The presence of nonstructural cracks reduces the punching capacity of the slab.

The comparison of the values of the ultimate load carrying capacity for good panels with low steel and for good panels with high steel shows the effect of the increased amount of steel. The tension steel for high steel panels (GH) was almost twice the amount of steel for low steel panels (GL). This increase in tension steel by about 100% has resulted in only about 14% increase in punching load. This favourable influence of tension steel in increasing the punching capacity has also been confirmed in earlier studies (3, 6).

The results of static tests using a bearing area of 100 x 200 mm (4 x 8 in.) are presented in Table 4.3. A comparison of these with those for the smaller bearing area

Table 4.2: Adjusted Static Tests Results Using a Bearing Area of 50 x 100 mm.

Panel Type	Avg. Core Strength (N/mm^2)	Avg. Failure Load (KN)	Failure Load Adjusted to f'_c = 19.8 N/mm^2	ACI (KN) Punching Load
BL	19.80	97	97	76
GL	17.70	115	122	72
GH	17.70	138	147	72

(Table 4.1) shows that the ultimate punching load increases with the increase in loaded area as expected. The result also confirms what was deduced earlier that the load carrying capacity of badly constructed panels is adversely influenced by initial flaws in construction. This may not be evident for panel GL1/2 which failed at a lower load than BL3/1 but this happened as a result of the low concrete strength of GL1/2. If the panel of good construction had the same strength as BL3/1, the failure load would have been higher. Using a correction factor as defined earlier, the value of Pu can be estimated as 152 KN for identical concrete strength. Thus, it can be concluded that in general punching load capacity of good panels was higher than that of bad panels under the increased loaded area of 100 x 200 mm.

Two static tests on BL panels in Table 4.3 were conducted using different orientation of the bearing plate to examine if the orientation of the rectangular loaded area would significantly influence the value of Pu. For the panel BL3/1, the longer dimension of the bearing plate was parallel to the girder, while in the other panel, BL4/2 the longer dimension of the bearing plate was perpendicular to the girders. Test results show that the orientation of the bearing plate had little effect on the punching load.

The ultimate flexural capacity of these panels (given

Table 4.3: Static Tests for Restrained Panels Using a Bearing Area of 100 x 200mm

Panel	Core Strength (N/mm^2)	Failure Load (KN)	ACI Punching Load (KN)
BL3/1	19.9	139	114
BL4/2	21.4	141	118
GL1/2	14.0	128	90
GH4/1	18.3	147	108

in Chapter 3) is greater than the failure load of these slabs in static tests which means that the slab did not by any means exhibit any premature flexural failure.

As shown in Tables 4.1 and 4.3 the computed ACI punching failure loads are consistently lower than the experimental values, indicating the conservative nature of the formula prescribed in reference (25) which ignores the favourable influence of the dowel action of rebars which contributes to the enhancement of the failure load. The ratio of the ACI punching loads to the experimental values ranged from a maximum value of 0.84 to a minimum value of 0.46.

The failure pattern of the panels in static tests shown in Plates 4.1 and 4.2 depicts a hole of the size of the bearing area at the top and a larger dislocated area at the bottom. The fractured area of concrete resembles a conical shape. At the early stage of loading (about 20-30 KN), a few longitudinal cracks caused by flexure are observed at the bottom. With increased loading, these cracks become predominant with larger widths and lengths and more new cracks develop radiating from the loaded zone. Prior to fracture, extensive cracking of the underside of the slab is noticed with cracks diverging in all directions from the central region. The failure is associated with a large dislocated area at the bottom, extending almost the full

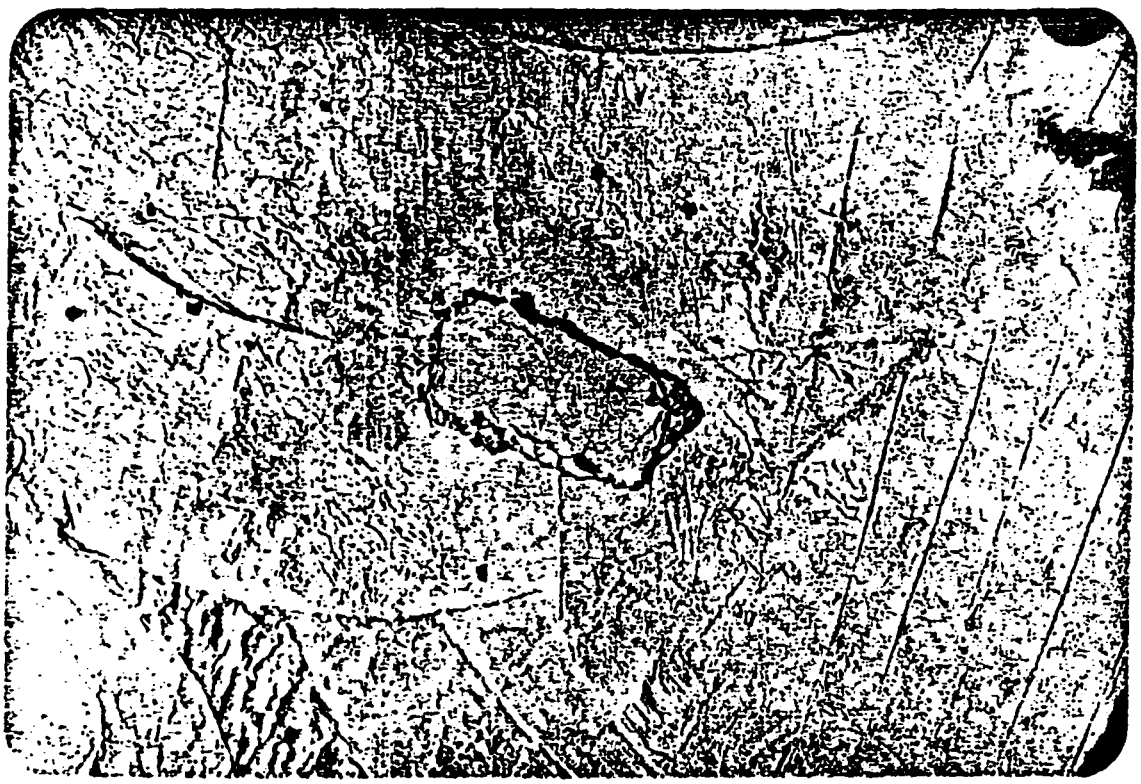

Plate 4.1a: Top of Slab After Failure

Plate 4.1B; Bottom of Slab After Failure

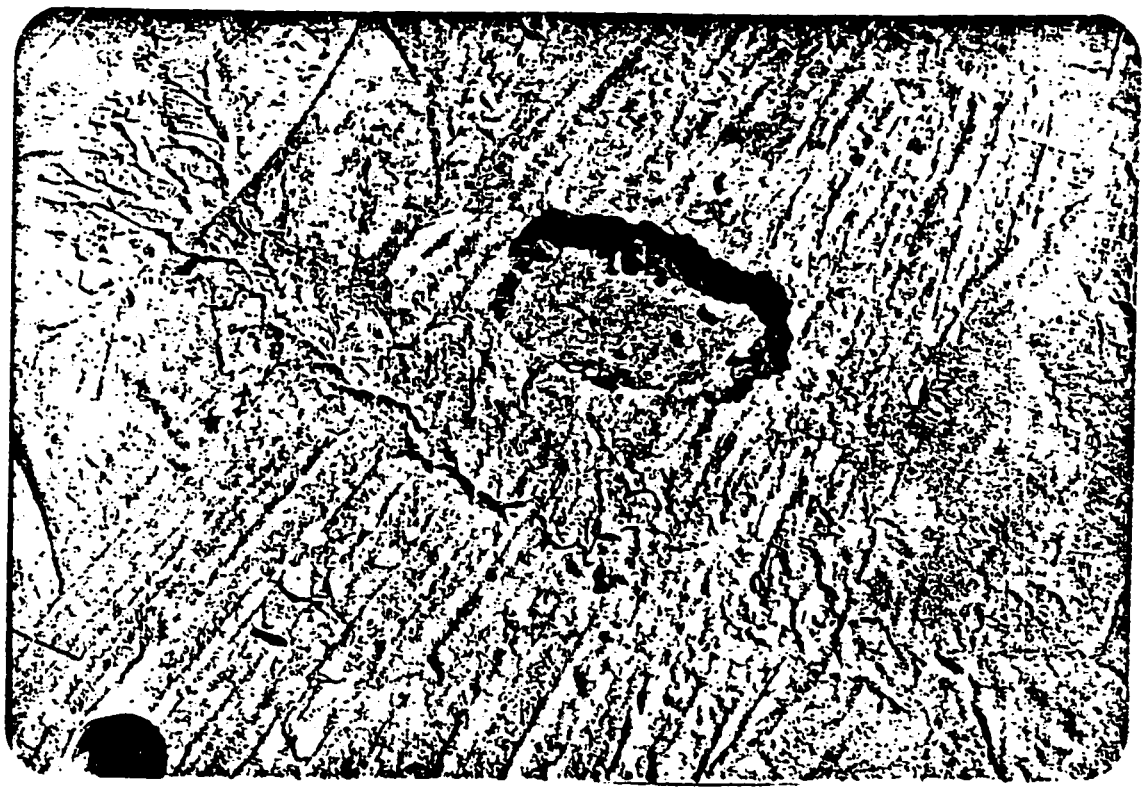

Plate 4.2a: Top of Slab After Failure

Plate 4.2b: Bottom of Slab After Failure

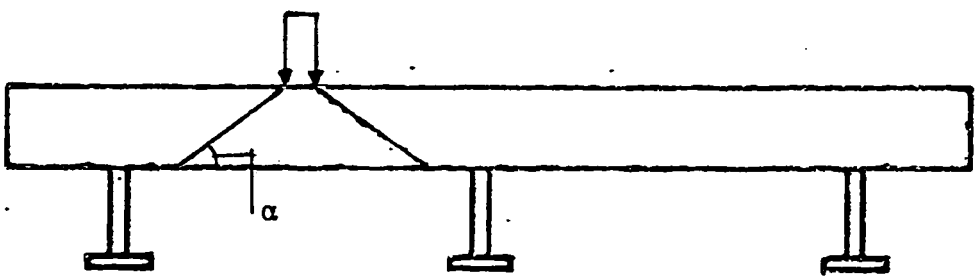

Fig. 4.1: Failed Cone of Concrete

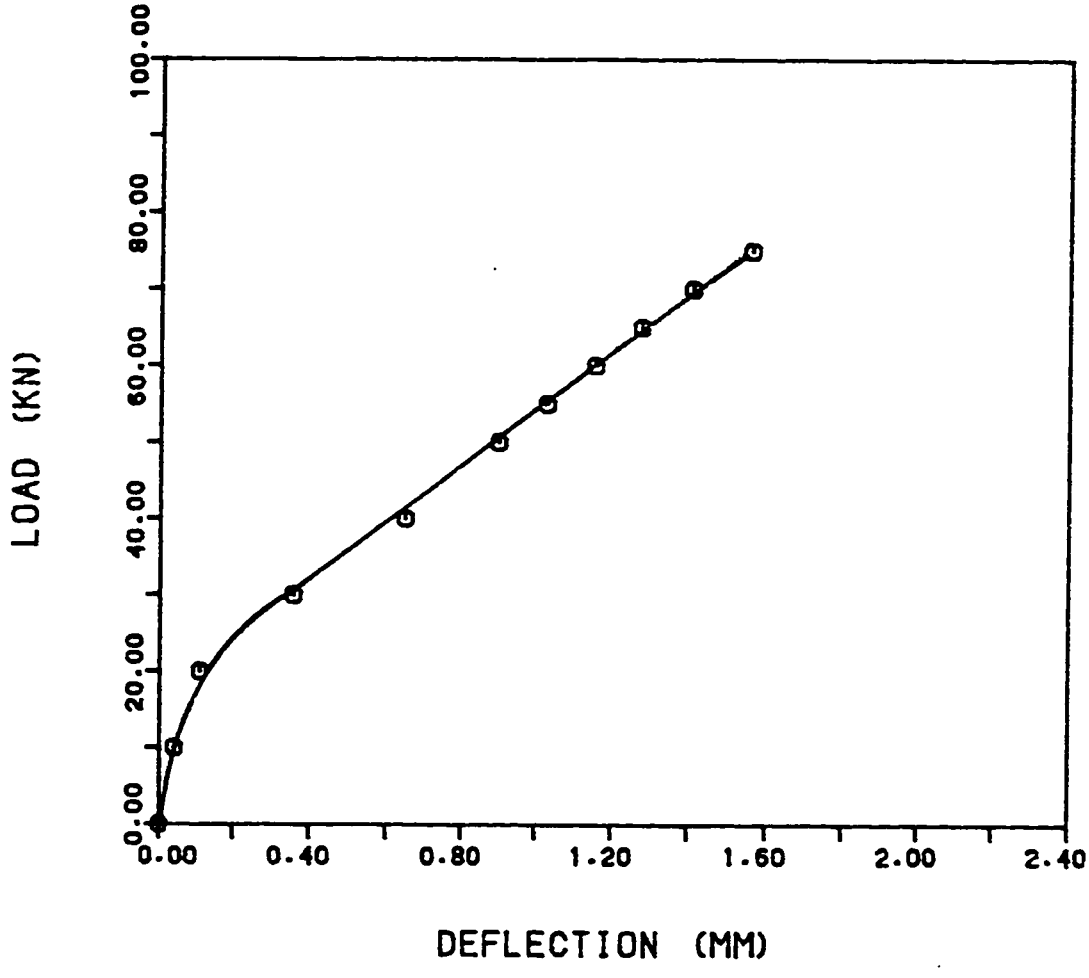

Fig. 4.2: Load Deflection Response for Panel GL4/1.

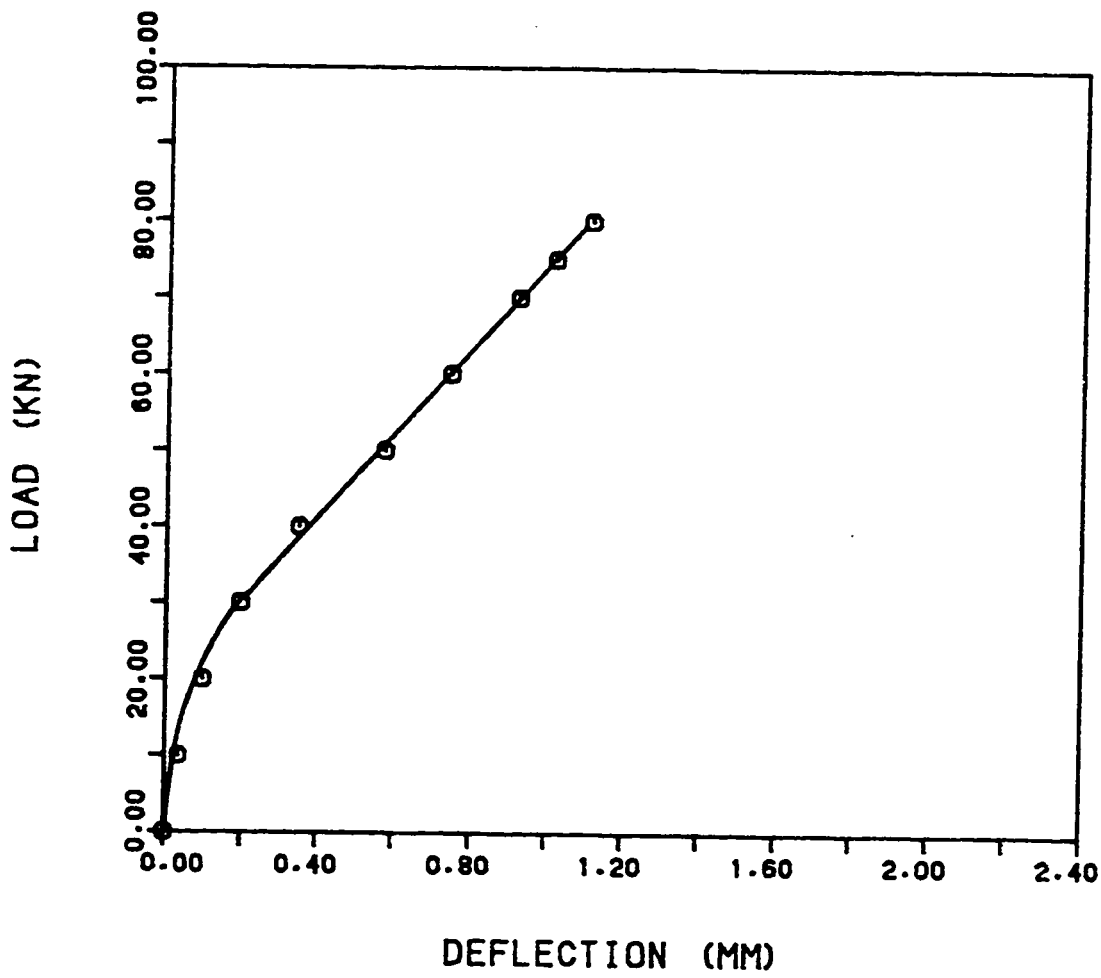

Fig. 4.3: Load Deflection Response for Panel BL4/2.

span of the slab between girders. The approximate size of the bottom area of the fractured concrete was measured. The results showed that this area is consistently greater for panels with high steel and also this area increased as the loaded is increased. The angle of concrete cone (α) (Fig. 4.1) ranged from a minimum of 22^{o} to a maximum of 28^{o}.

The deflection for some panels was measured using three dial gages to observe the load-deflection response for the slab. These dial gages were used to record the deflection at: (i) the center of the edge beam, (ii) the center of the middle beam and (iii) the center of loaded area. The load-deflection relationships for two panels are shown in Figures 4.2 and 4.3. The horizontal axis represents the center of slab deflection which was computed by subtracting the average deflection of the two supporting beams from the deflection of the slab at the load point. During the early stages of loading the deck behaved relatively stiffer and after a load of about 25 KN the system stabilized and its compliance increased a little due to increased flexural cracks. It is worthy to note that the load-deflection plot shows almost a linear relationship upto about 80% of the failure load. No measurements were recorded at higher load levels as the dial gages were withdrawn to prevent them from being damaged due to sudden failure of the slab.

4.1.2 *Fatigue Tests*:

For all fatigue tests conducted on restrained panels, a constant stress (load) ratio of about 0.1 was used. Also a loaded area of 50 x 100 mm (2 x 4 in.) was used in all tests, since this assured a punching shear type failure at lesser load level. Under these conditions, the fatigue life of restrained slabs was determined for various load levels greater than 0.6 Pu since fatigue test at load levels smaller than 0.6 Pu yielded no failure in less than two million cycles.

Test data generated for the three types of restrained slabs, namely BL, GL and GH are shown in Tables 4.4 to 4.6. Due to small variation of concrete strength for panels, the result of the static tests cannot be taken as the ultimate capacity of all panels. Instead the ultimate strengths were predicted by using the correction factor based on core compressive strength as discussed earlier. The maximum fatigue load P can be nondimensionalized by dividing the loads with the static ultimate capacity Pu. Data presented in Tables 4.4 to 4.6 can then be converted to data relating P/Pu to N as shown in Table 4.7. Data generated for each type of panels are shown in a conventional semi-log plot of S-N (load versus number of cycles to failure) diagram in Figures 4.4 to 4.6. These graphs can be combined into one

Table 4.4: Fatigue Data for BL Panels

Panel	Core Strength	Maximum Load	Cycles
BL1/1	19.9	97	1 (Static)
BL4/1	17.3	85	2,870
BL1/2	18.5	80	32,600
BL2/1	18.8	70	101,050
BL2/2	18.8	60	No Failure

Table 4.5: Fatigue Data for GL Panels

Panel	Core Strength (N/mm^2)	Maximum Load (KN)	Cycles
GL1/1	17.7	115	1(Static)
GL4/2	20.9	111	1,320
GL2/2	16.8	90	44,600
GL2/1	16.8	80	540,750

Table 4.6: Fatigue Data for GH Panels

Panel	Core Strength	Maximum Load	Cycles
GH1/1	17.7	139	1(Static)
GH1/2	15.3	120	240
GH3/2	14.1	100	3,630
GH3/1	14.1	85	293,000

Table 4.7: Fatigue Results for Restrained Panels.

Panel Type	P/Pu	N
BL	1.0	1 (Static)
	0.9	2,870
	0.85	33,000
	0.76	101,050
	0.6	No Failure
GL	1.0	1 (Static)
	0.9	1,320
	0.8	45,000
	0.7	541,000
GH	1.0	1 (Static)
	0.93	240
	0.81	4,000
	0.7	293,000

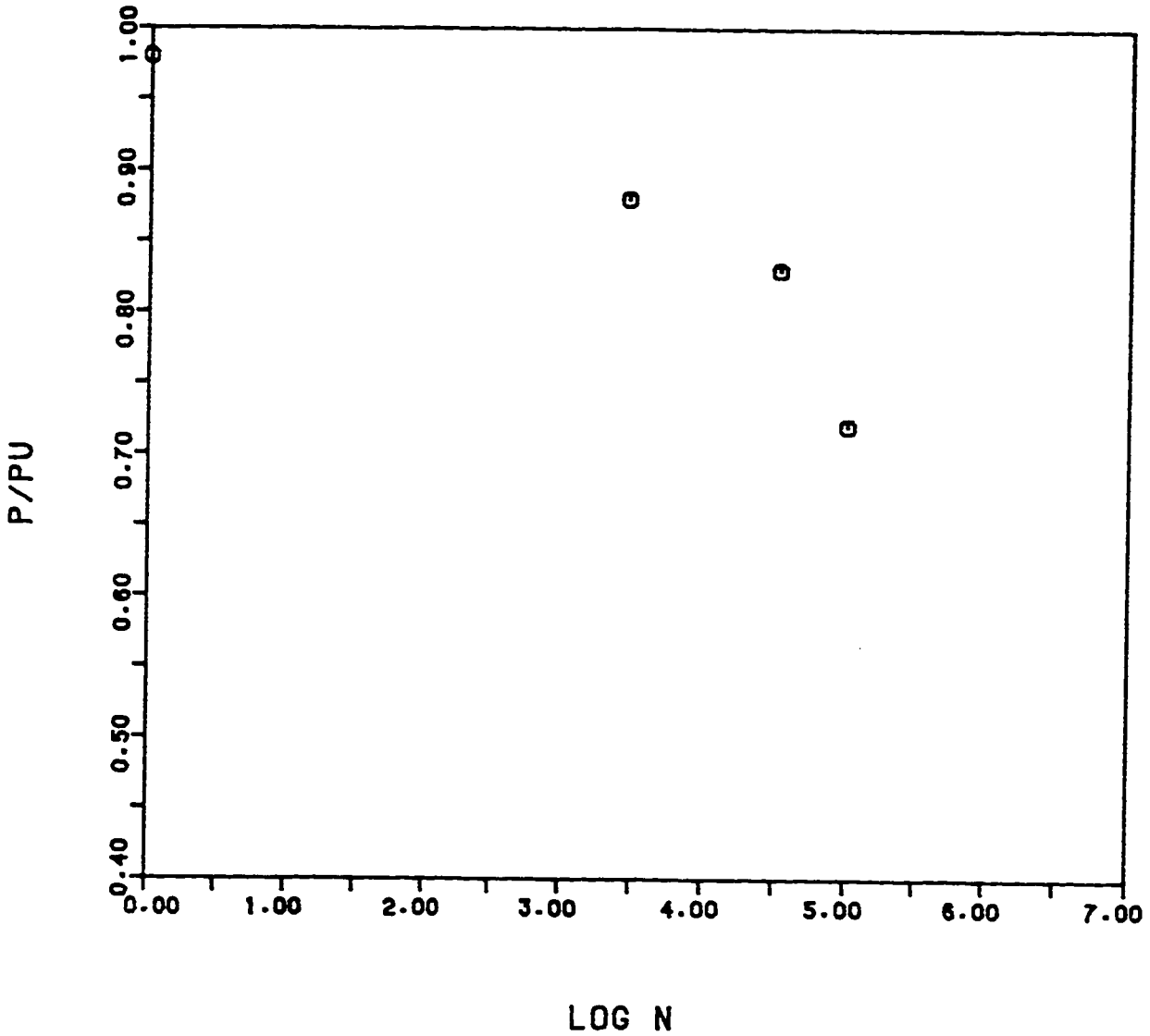

Fig. 4.4: S-N Diagram for BL Panels.

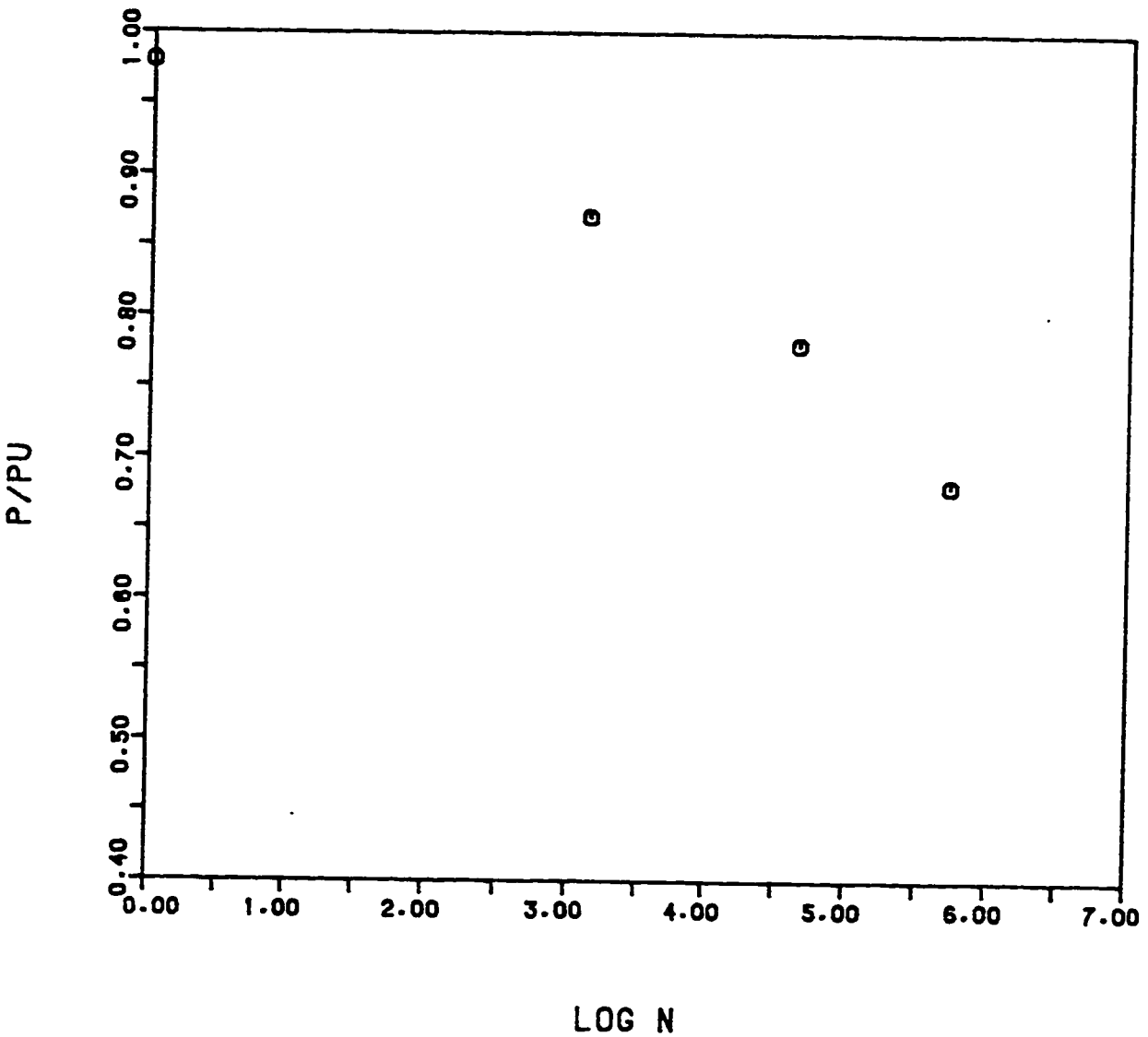

Fig. 4.5: S-N Diagram for GL Panels.

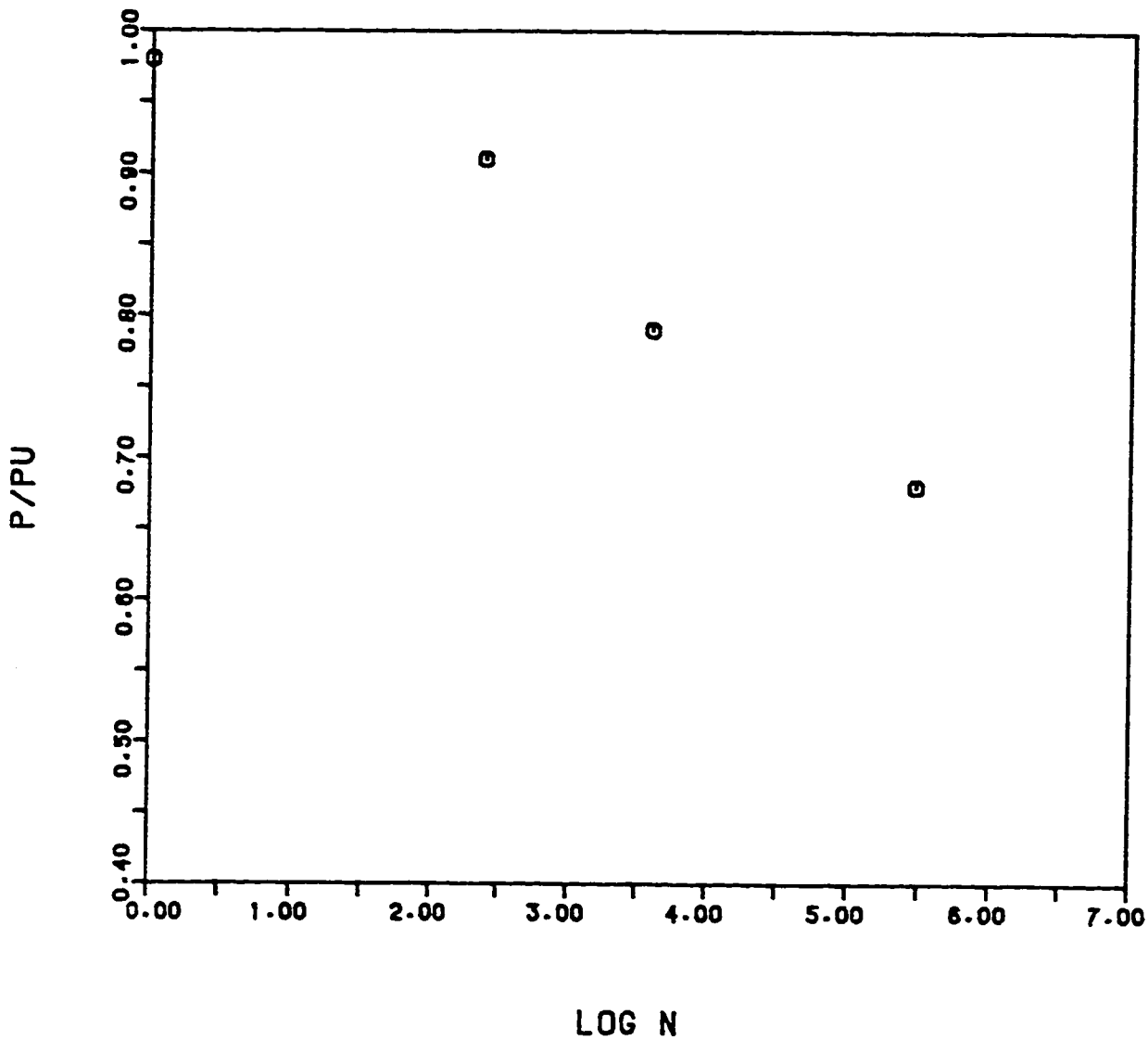

Fig. 4.6: S-N Diagram for GH Panels.

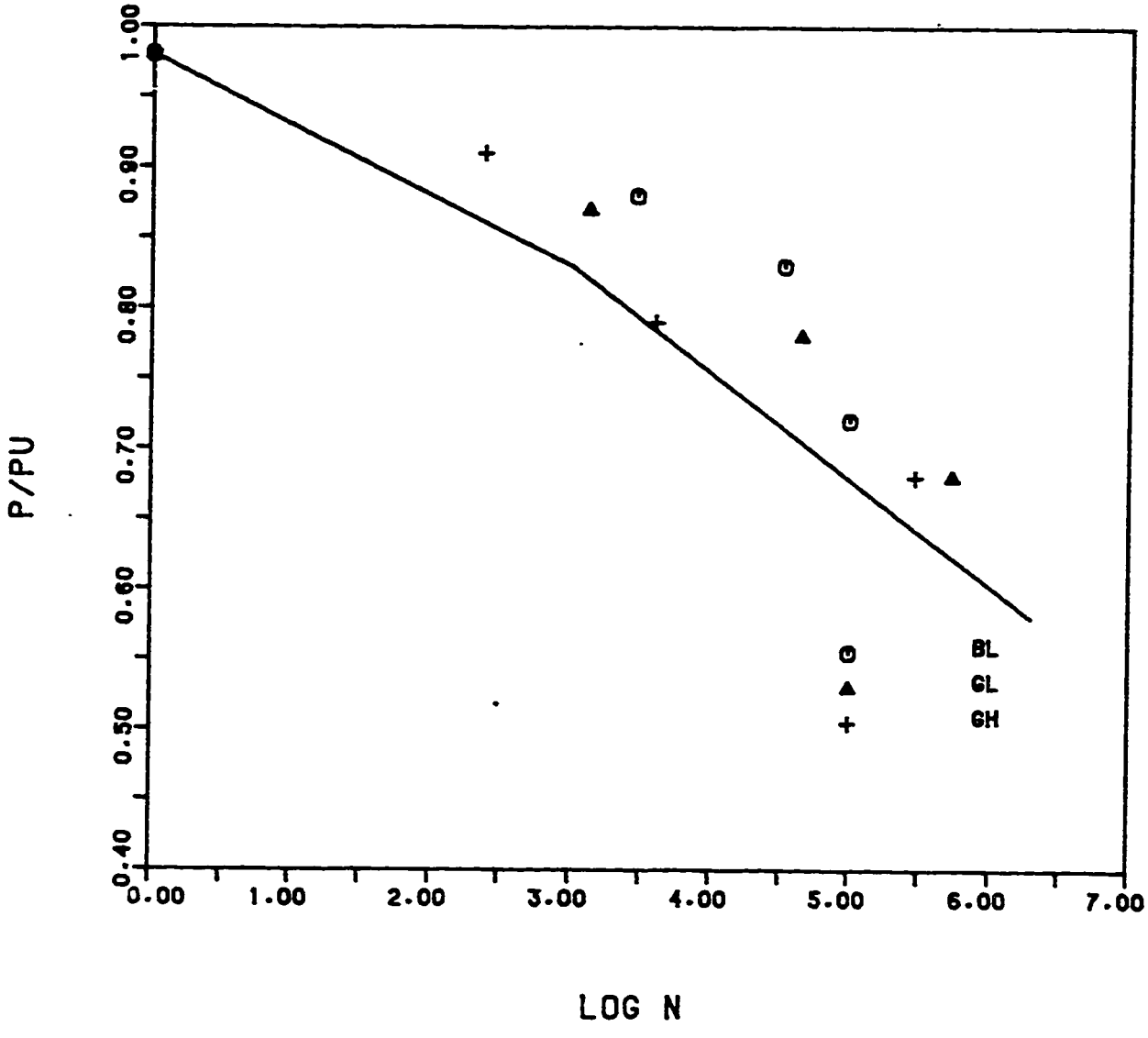

Fig. 4.7: S-N Diagram for Restrained Panels.

plot to show collectively all test data generated for all panels. Fig. 4.6 represents such a plot of all data. An attempt has been made to safely predict the fatigue life using these data. Taking into account the implicit requirement of a safe prediction of fatigue life, the proposed bi-linear relationship shown in Fig. 4.7 reasonably correlate the data points within the range of N values considered in this test.

It is of interest to note that the proposed P/Pu versus N plot is independent of the specimen type, i.e. it is valid for both good and bad panels. However, this does not imply that the life of a panel with construction relatd cracks is identical to that of a perfect panel. The difference exists in the magnitude of the load level, as for the same P/Pu, the maximum applied load on a bad panel would be less than that on a good panel. The relation between P/Pu and N for a stress ratio of 0.1 as depicted in Figure 4.7, can be expressed as:

$$P/Pu = 1.0-0.05\ \text{LogN} \quad N<10^3 \quad \text{.....(4.1a)}$$

$$P/Pu = 1.077-0.0758\ \text{LogN} \quad 10^3<N<2 \times 10^6 \text{.....(4.1b)}$$

As tests revealed that the fatigue failure of a panel is unlikely to occur below 2×10^6 cycles with a maximum load level less than 60% of the static capacity, a value of P =0.5 Pu can safely be considered as a threshold level for

punching type fatigue failure in design of bridge deck slabs. It should be emphasized that the test data were generated using a loaded area of 50 x 100 mm (2 x 4 in.) which ensured punching failure.

The fatigue failure under a small patch load can be characterized by a sudden fracture of a conical area of concrete from the deck by successive nucleation and propagation of cracks. As number of cycles grows, cracks at the bottom become wider and well formed and more cracks are seen to appear from the central loaded zone radiating in all directions. While the top part of the dislocated concrete matches the bearing area, the bottom part is considerably larger in area. Failure pattern is essentially similar to those observed in static tests (Plates 4.1 and 4.2).

4.2 Unrestrained Panels

These panels are categorized into four groups according to the amount of reinforcement and the curing conditions. These groups are: (i) good construction with high steel (UGH), (ii) bad construction with high steel (UBH), (iii) good construction with low steel (UGL) and (iv) bad construction with low steel (UBL). On these panels static and fatigue tests were carried out using a patch loads area of 32 x 64 mm (1.25 x 2.5 in.). Fortunately the variation of compressive strength for the panels was very small since

the same materials and mix design were used for all these panels. The test results and findings are presented in the following sections.

4.2.1 *Static Tests*

One panel of each group was tested to evaluate the static capacity. The results are shown in Table 4.9 along with the flexural capacity of unrestrained panels. The theoretical punching load obtained in Chapter 3 and the ACI punching load. In all tests, the failure of slabs portrayed punching type failures. A typical panel after failure is shown in Plate 4.3. The ultimate load to cause flexure failure was calculated in Chapter 3 from a yield-line analysis. These values are given in Table 4.8. The load to induce bending failure was greater than the slab failure loads in static tests, thus ruling out any premature flexure failure. The edge shear stress on a reasonable effective slab width showed stress level less than critical values specified by ACI.

Table 4.8 shows that the punching load predicted by ACI was considerably lower than the test values in all cases, the minimum difference being of the order of 20%. Comparison of Pu values for high and low steel panels shows that the panels with higher amount of main steel yielded larger Pu indicating the favourable influence of tension

Table 4.8: Static Tests for Unrestrained Panels

Panel	Concrete Strength (N/mm)	Ultimate Load (kN)	Flexural Capacity (kN)	ACI Punching Load (kN)	Theoretical Punching Load *
UBH1	19.0	59	110	32	39
UGH1	21.0	57	110	33	43
UBL1	18.0	42	60	31	37
UGL1	17.0	41	60	30	35

*Using Plasticity Approach

steel in increasing the punching capacity due primarily to the increased dowel action.

The theoretical punching loads are less than the experimental values for all four panels the ratio ranged from a minimum value of 0.66 to a maximum of 0.888. The plasticity approach by which the theoretical load was obtained ignores the favourable influence of tension reinforcement on the punching capacity of slabs.

Examining Table 4.8 one would conclude that the ultimate load carrying capacity is almost independent of the casting and curing conditions which contradicts the findings for restrained panels. This is due to the fact that it was not possible to create significant non-structural precracks in these small panels due to the small size of the specimens. Thus panels of both good and bad construction behaved almost identically. One may conclude that the effect of construction flaws are reflected more in relatively large size structures.

For three panels the strain in the embedded rebars was measured using strain gages to examine the stress in rebars. A plot of the load versus strain in the middle bar which lies under the patch load is shown in Figs. 4.8 to 4.10. From these figures it can be deduced that the middle bar yielded when the load reached about 75% of the ultimate capacity of the slab.

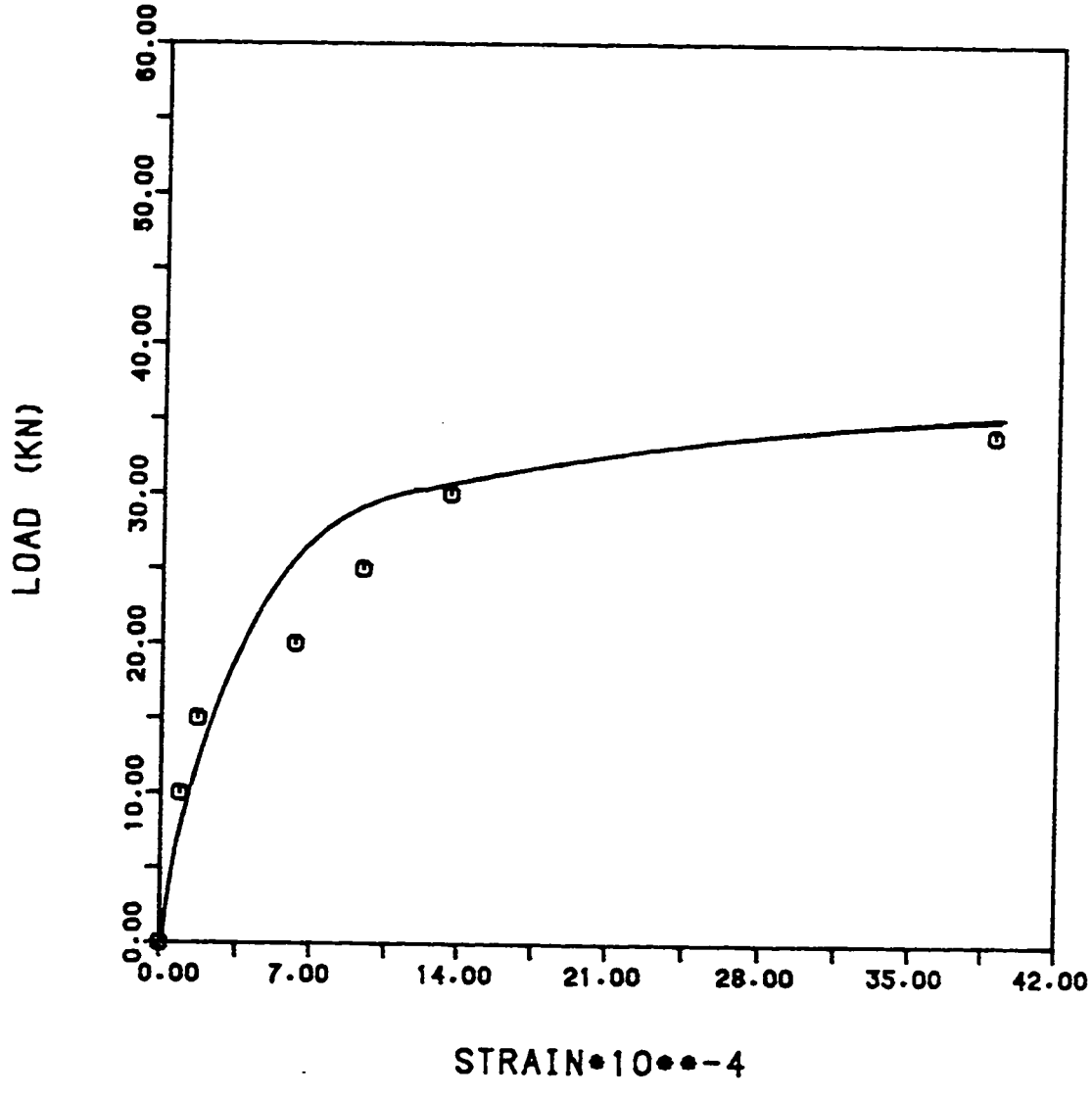

Fig. 4.8: Load-Strain Relationship for Middle Rebar in UBL4.

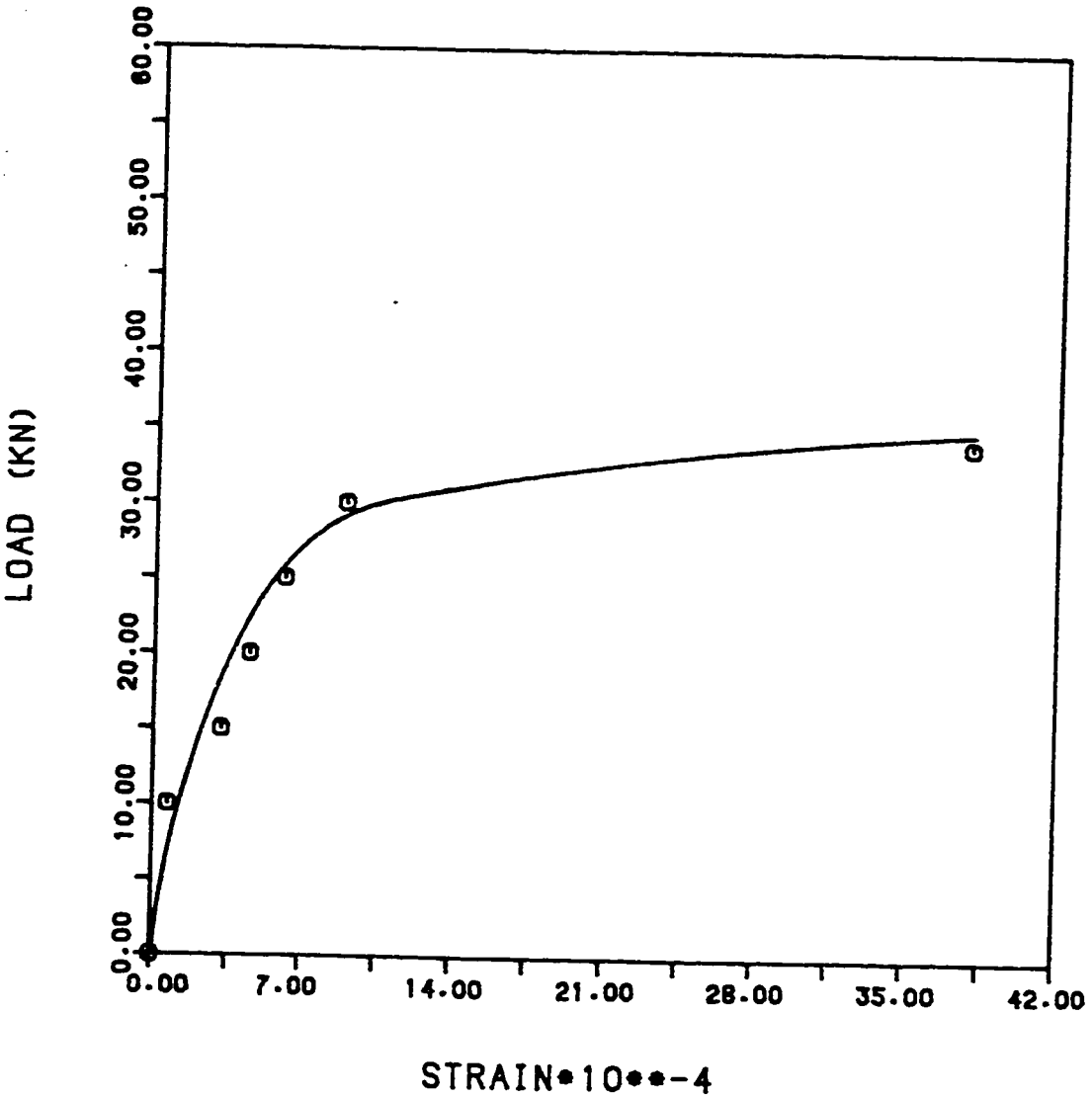

Fig. 4.9: Load-Strain Relationship for Middle Rebar in UGL4.

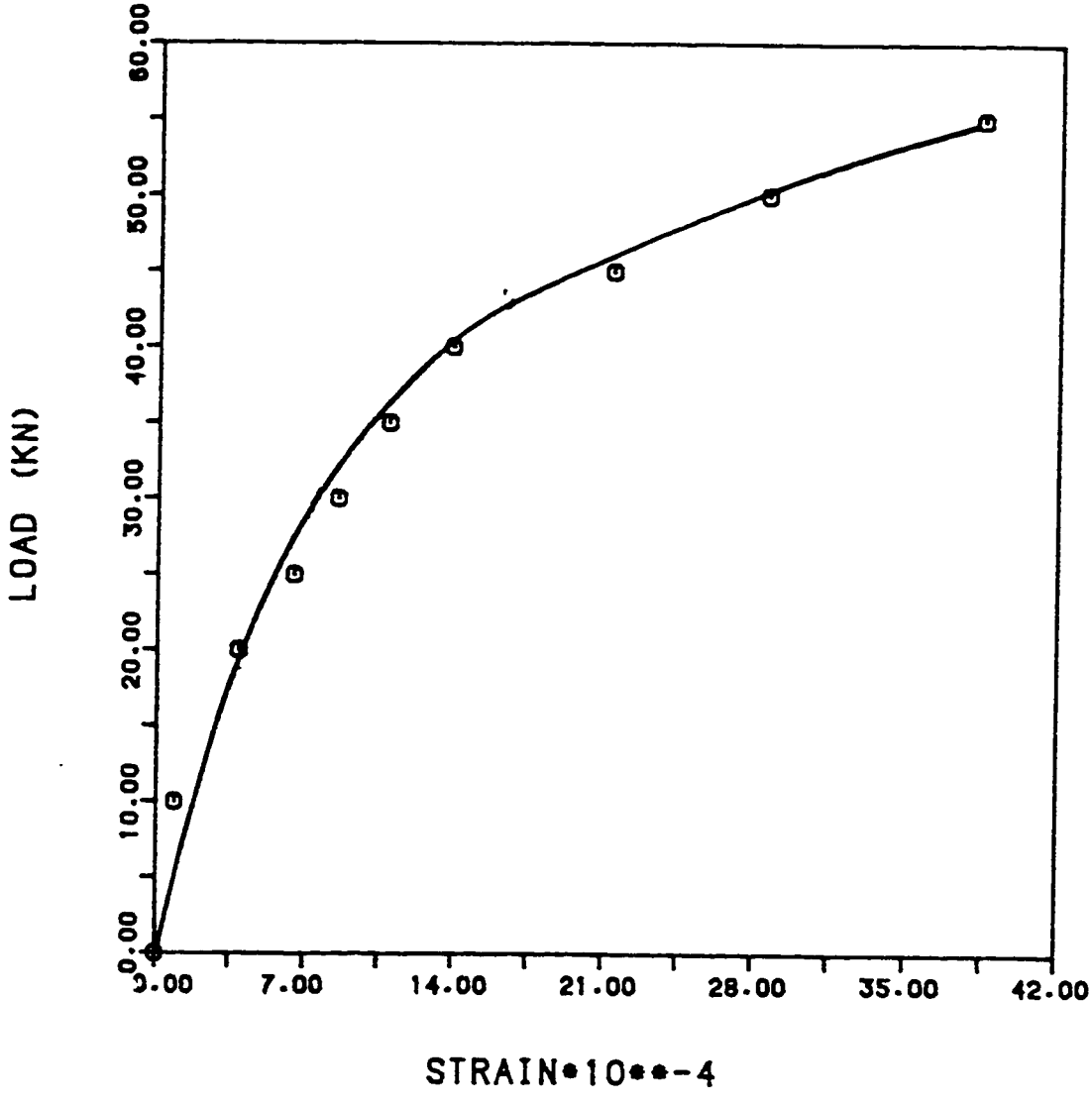

Fig. 4.10: Load-Strain Relationship for Middle Rebar in UGH1.

To measure the width of the slab which is most effective in resisting the applied load, an attempt was made to record strains in several bottom tension bars away from the central loaded area. Fig. 4.11 shows location of the bars for low steel panels whose strains were measured under monotonically increased patch loads. Figs. 4.12 and 4.13 show the plots of strains. For the panel with high steel, strain plot for four rebars whose locations are shown in Fig. 4.14 are depicted in Fig. 4.15. Results show that strains in the rebars decrease as one moves further from the loaded area, indicating lesser stress as expected. The middle bar reaches the yield point first followed by the adjacent rebars. As the steel in the vicinity of the loaded area undergoes plastic deformation with large straining, the adjacent rebars are stressed progressively to yield point, enabling wider slab to participate in load carrying action. To demonstrate the level of tensile stress at the mid point of each rebar, Table 4.9 is given for panel UGH1 at one-half of the failure load. Strains were converted to stresses using a modulus of elasticity of steel as 200 GPa (29 x 10 ksi) and idealizing rebar behaviour as elasticplastic with yield stress of 345 MPa (50 ksi), the latter value being determined from tension test. As shown in Table 4.9 the stress across the width falls rapidly confining the heavily stressed zone near the narrow control strip of the slab.

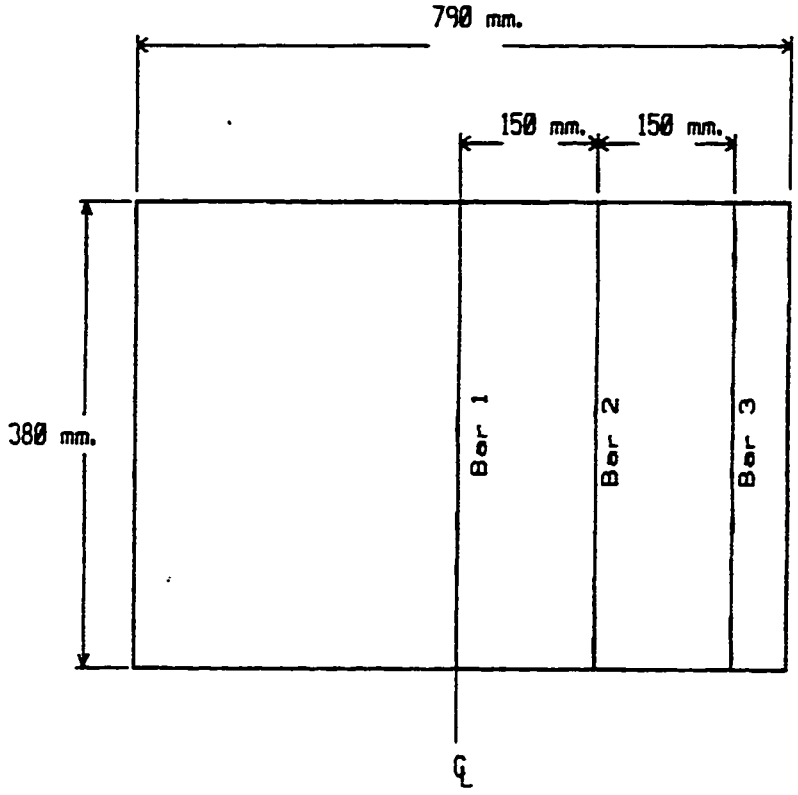

Fig. 4.11: Location of Rebars with Strain gages for low steel unrestrained panels.

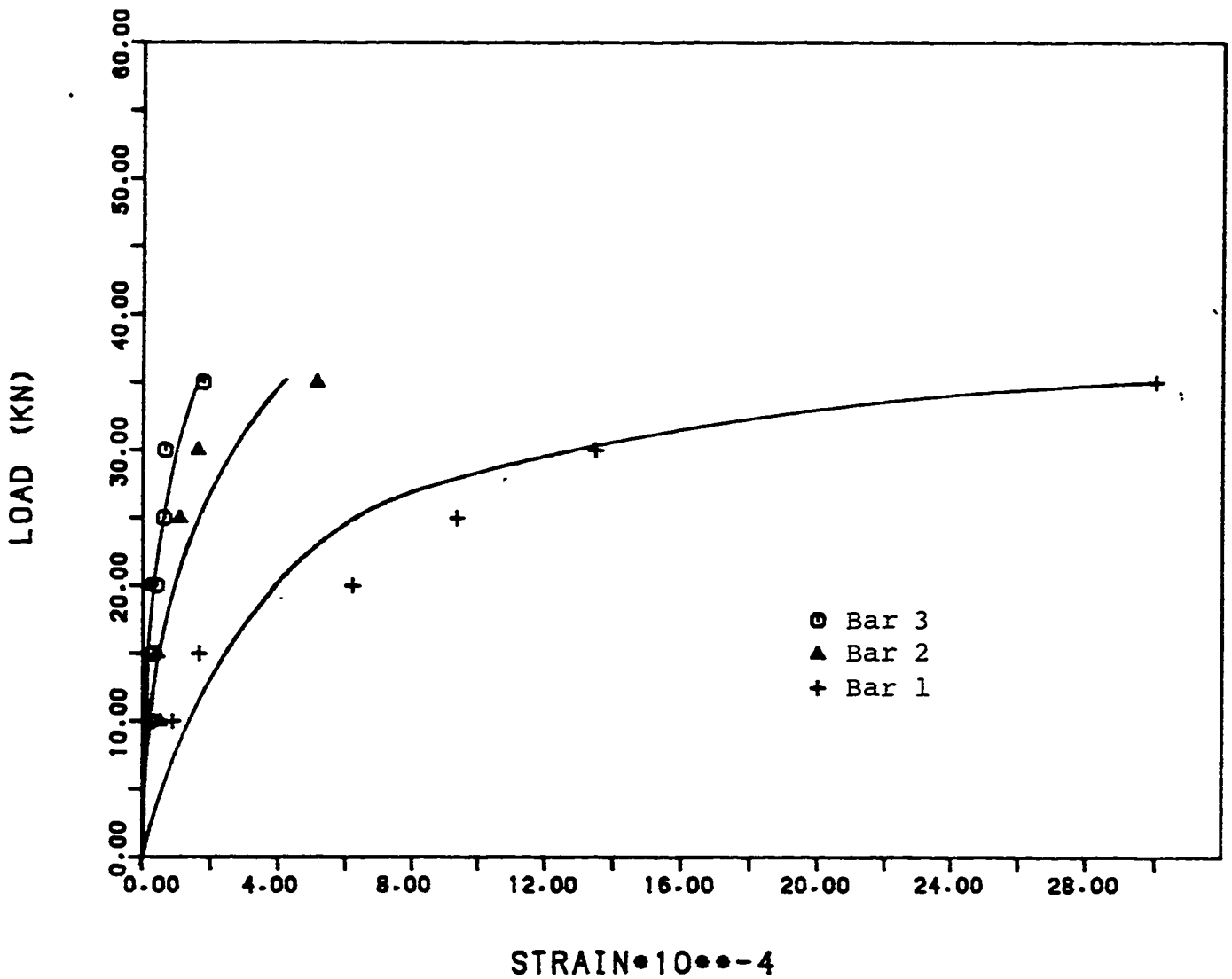

Fig. 4.12: Variation of Strain in Rebars of UBL4.

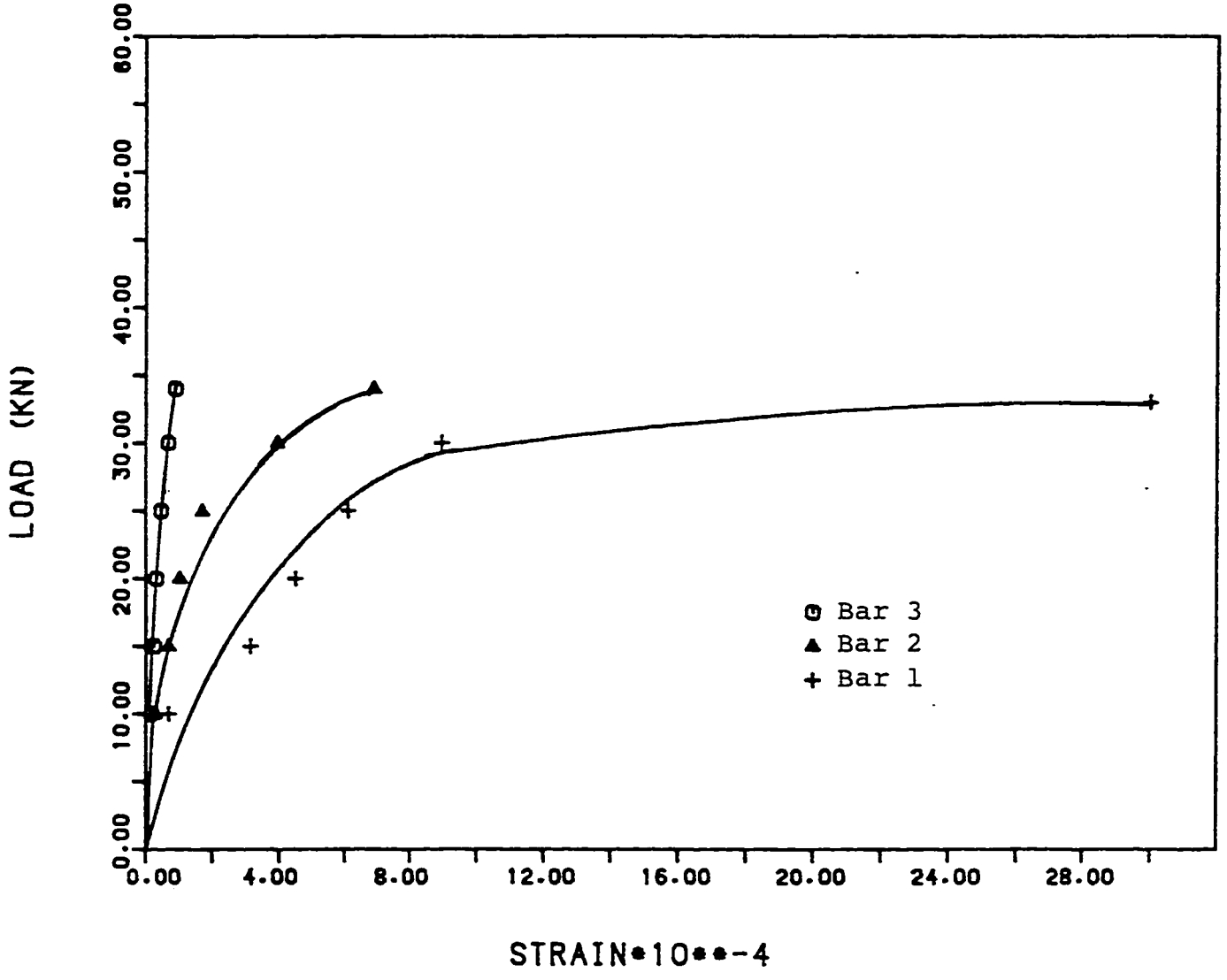

Fig. 4.13: Variation of Strain in Rebars of UGL4.

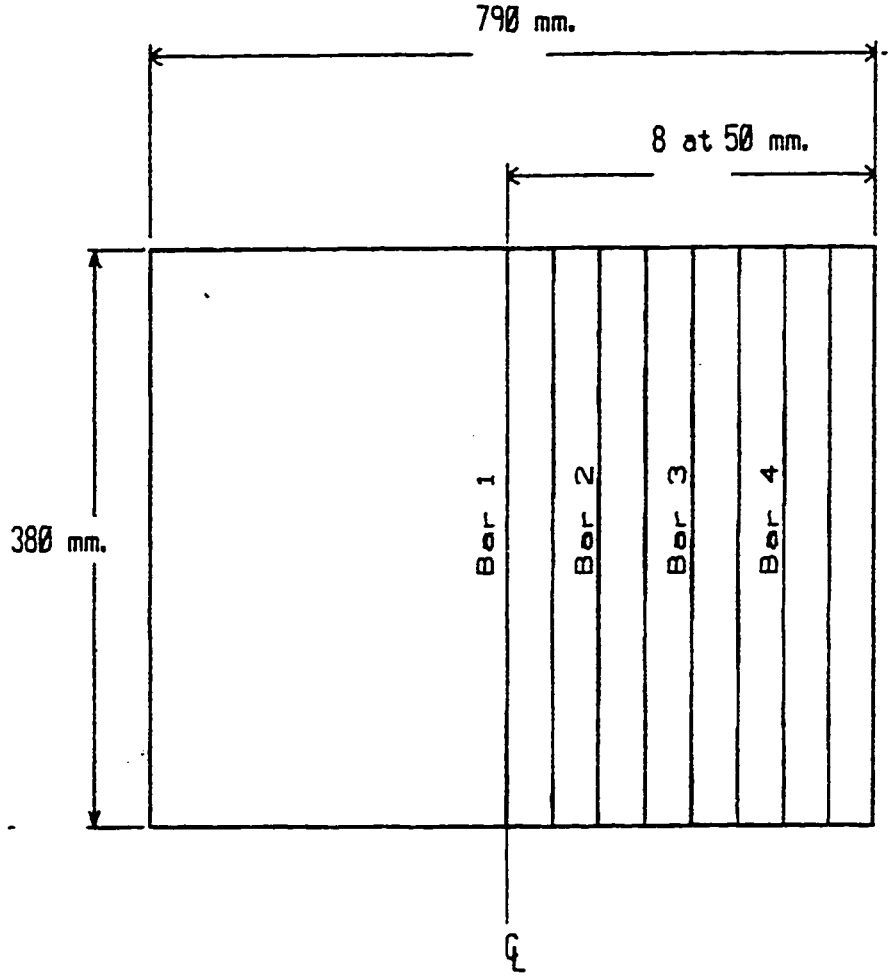

Fig. 4.14: Location of Rebars with Strain gages for high steel Unrestrained Panels.

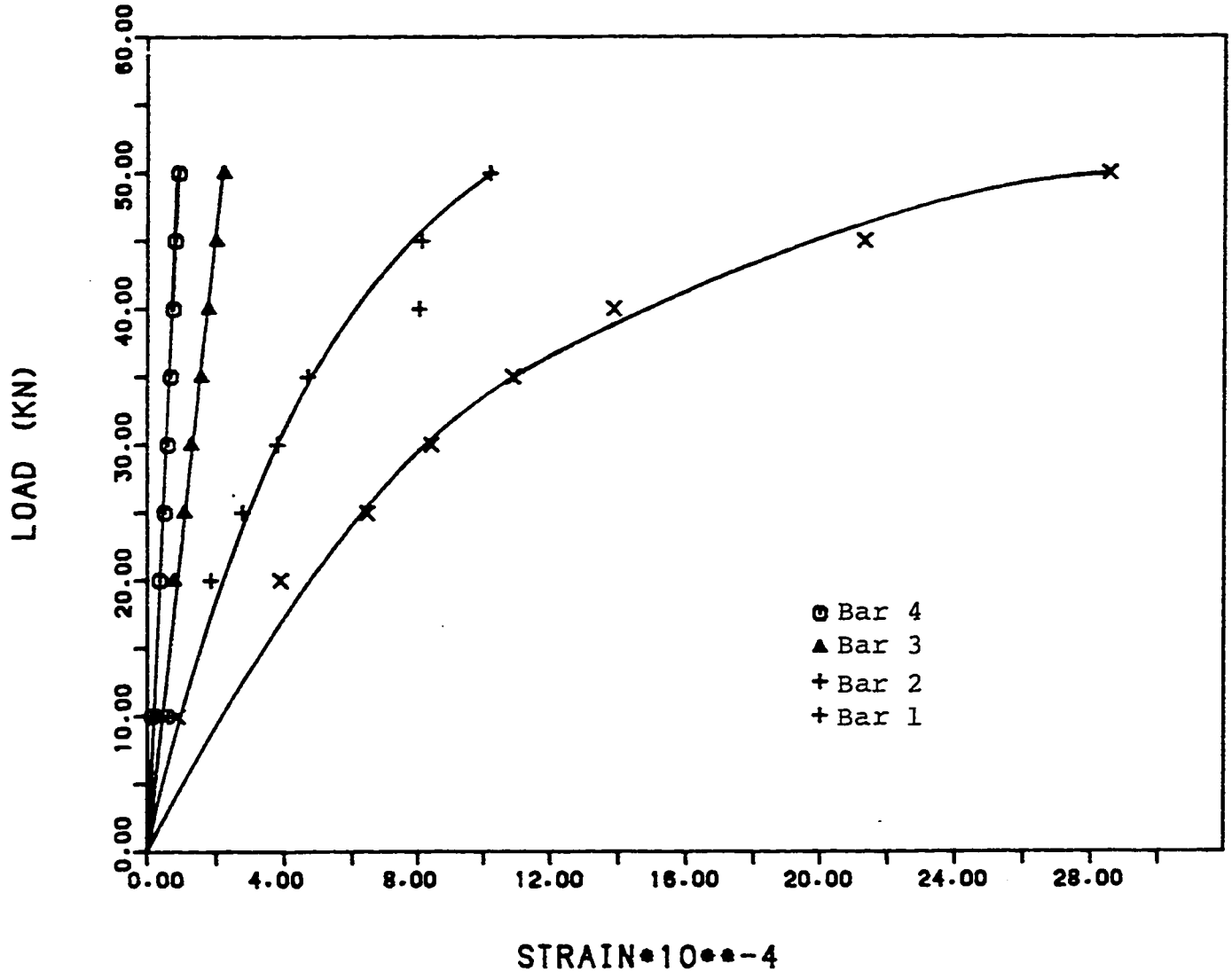

Fig. 4.15: Variation of Strain in Rebars of UGH1.

Table 4.9: Stresses in Rebars of Panel UGH1 at one-half the Ultimate Load

Rebar #	Stress (MPa)
Bar 1	168.2
Bar 2	75.8
Bar 3	25.5
Bar 4	11.7

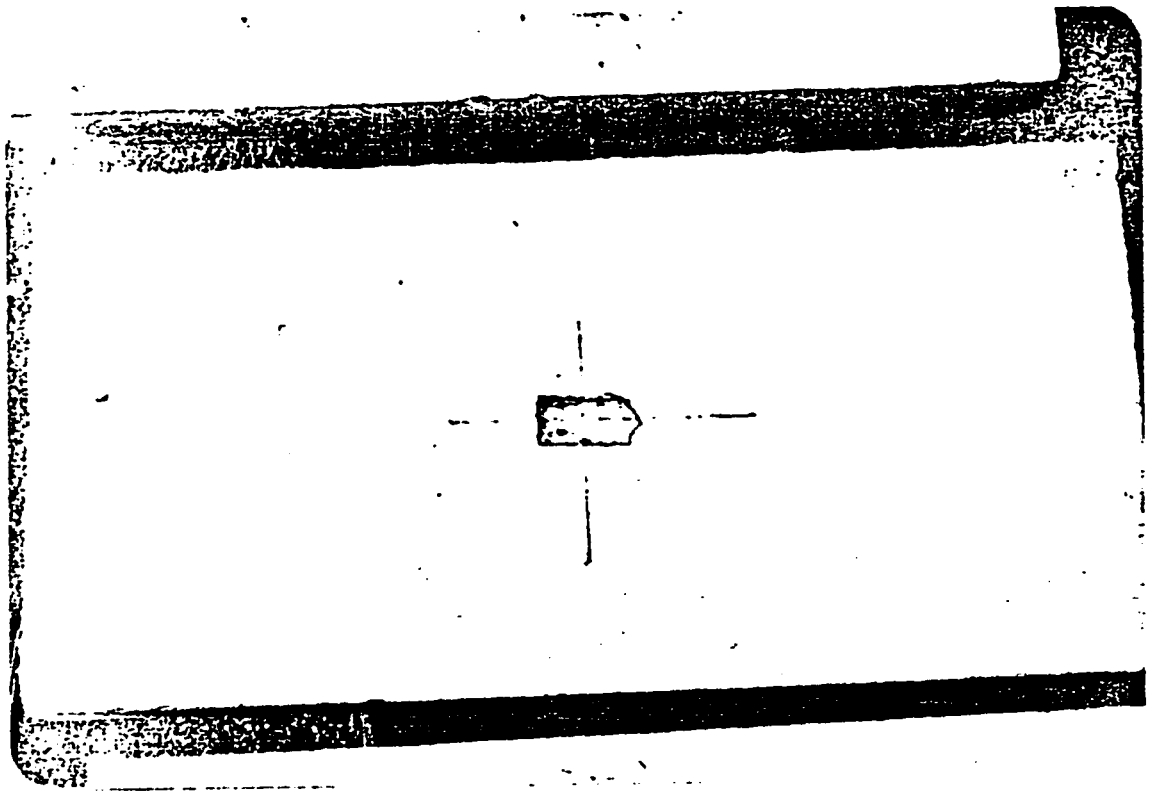

Plate 4.3a: Top of Unrestrained Slab after Failure.

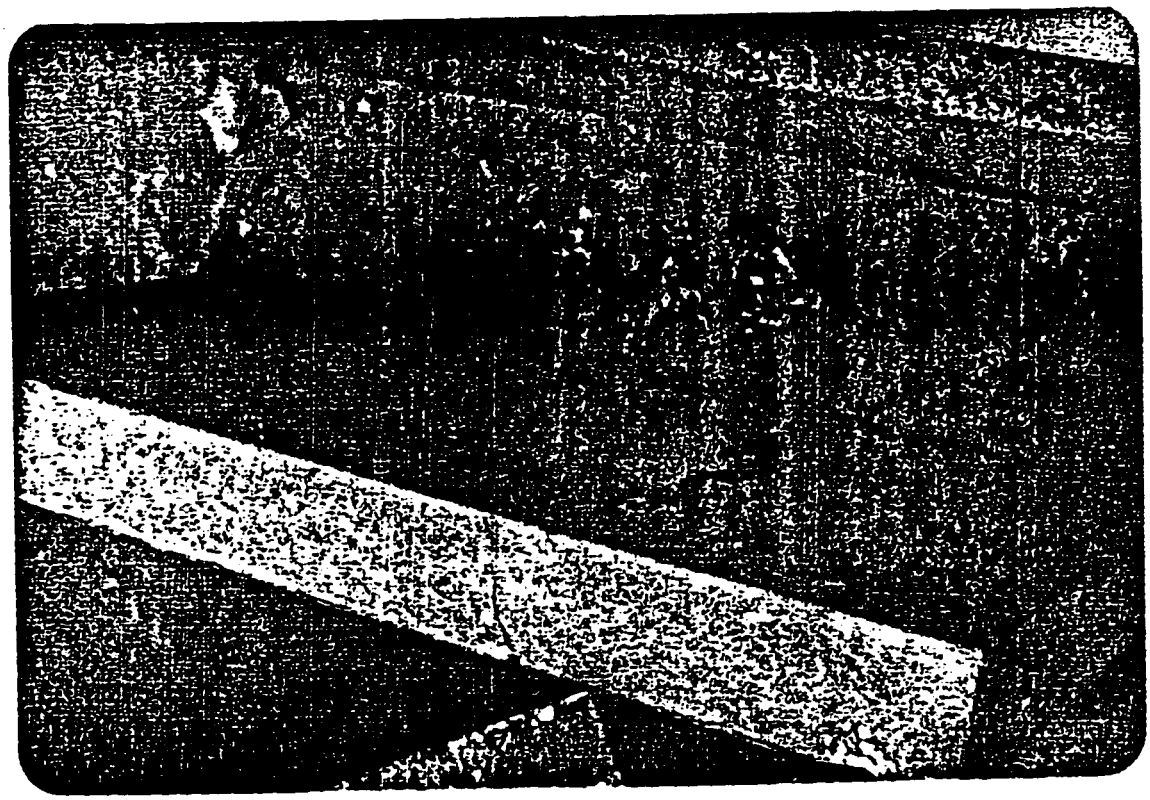

Plate 4.3b: Bottom of Unrestrained Slab after Failure

The ratio of the stress of bar No. 1 to that of bar No. 4 is 14.

The failure of these panels occurs with a dislocation of central concrete with a conical shape whose top matches the size of the bearing plate. At the bottom, the dislocation cover a larger area. A diagonal crack starts to form at the early stage of loading (about 10 kN) with further increase of loads radial cracks start to develop. These cracks become intensive and diverge in all directions before the concrete fractures.

4.2.2 *Fatigue Tests*

Fatigue tests on unrestrained slabs were carried out for different load levels keeping a constant stress ratio of about 0.1. Experimental data is shown in Tables 4.10 and 4.11 for the UB and UG panels, respectively. After non-dimensionalizing the maximum fatigue load by dividing it with the ultimate static capacity of the panels. the data of Tables 4.10 and 4.11 can be plotted in a non-dimensionalized plot relating P/Pu to number of cycles to failure N on a semi-log S-N diagram. Fig. 4.16 is S-N diagram for bad unrestrained panels while Fig. 4.17 is the S-N diagram for good unrestrained panels. These plots show that, in general, there is no sharp evidence of having distinctively different fatigue lives for panels with higher and lower

Table 4.10: Fatigue Data for Unrestrained Bad Panels

Panel	Maximum Load (kN)	P/Pu	Cycles to Failure
UBH1	59	1.0	1 (static)
UBH2	41	0.70	7,120
UBL1	42	1.0	1 (static)
UBL2	37	0.88	100
UBL3	34	0.80	4,000
UBL4	27	0.65	200,000

Table 4.11: Fatigue Data for Unrestrained Good Panels.

Panel	Max. Load (kN)	P/Pu	Cycles to Failure
UGH1	57	1.0	1 (static)
UGH2	51	0.90	120
UGH3	40	0.70	4,000
UGH4	37	0.65	147,900
UGL1	41	1.0	1 (static)
UGL2	37	0.90	1,300
UGL3	29	0.70	36,000
UGL4	27	0.65	75,900

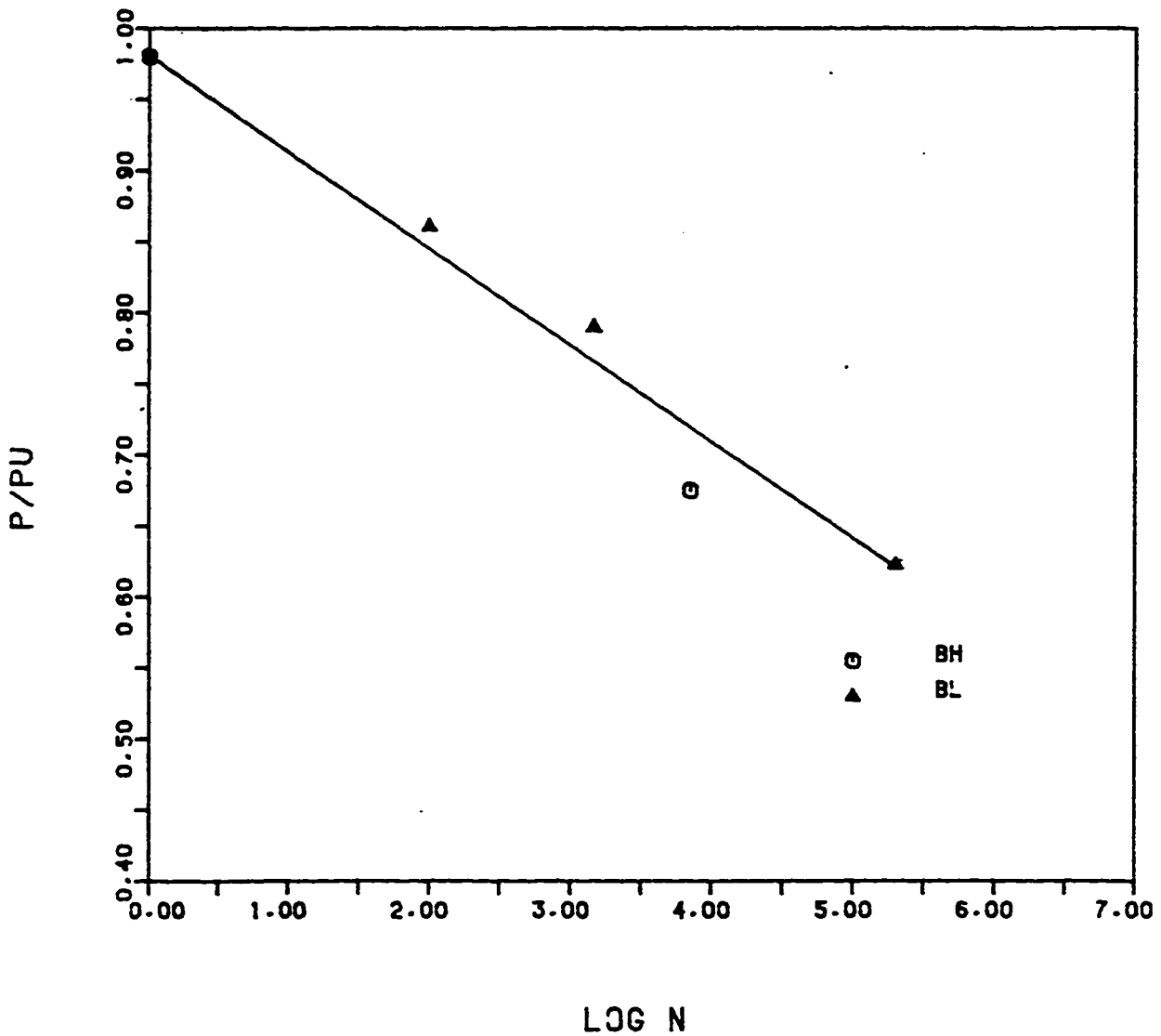

Fig. 4.16: S-N Diagram for Unrestrained Bad Panels.

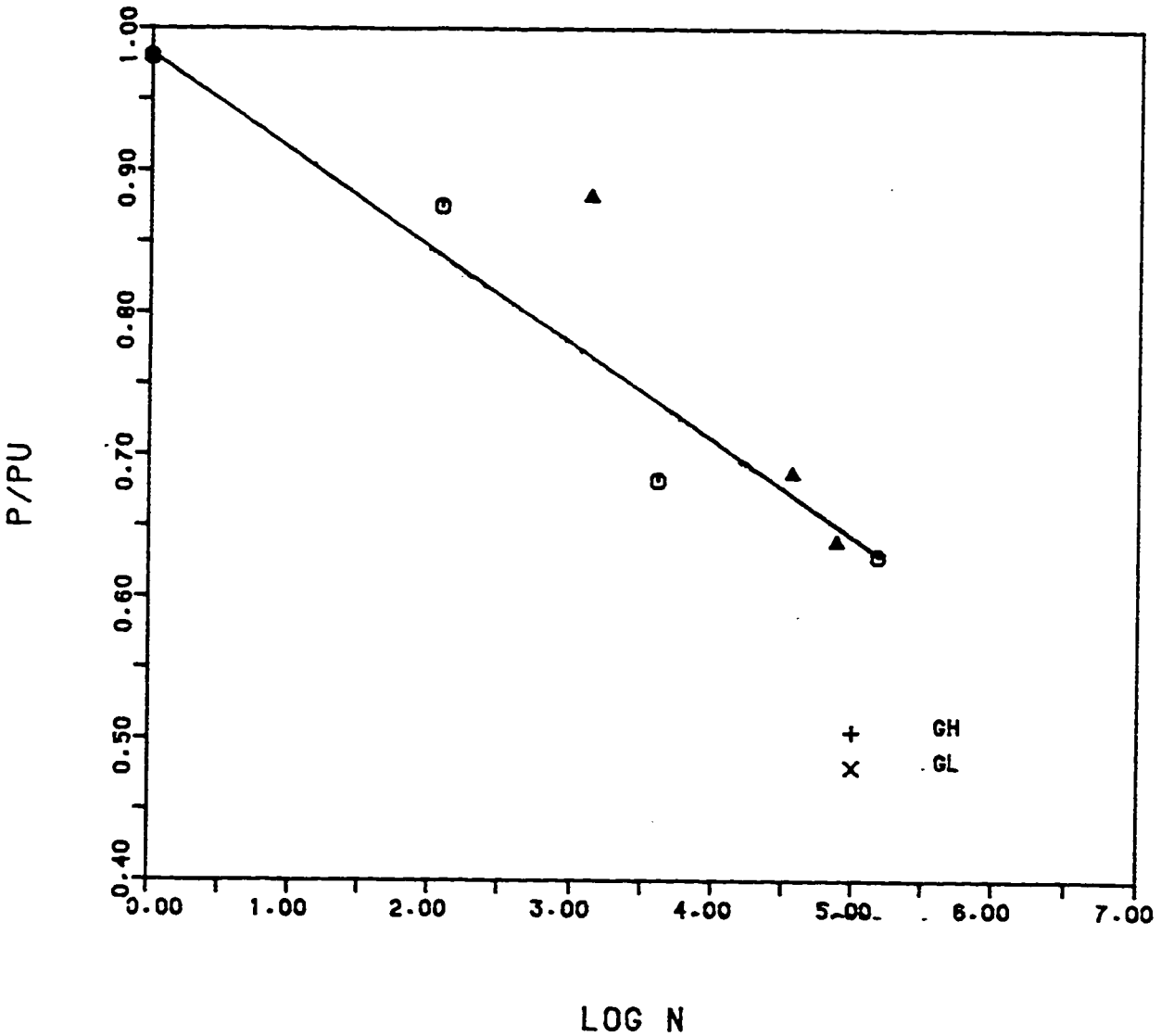

Fig. 4.17: S-N Diagram for Unrestrained Good Panels.

main steel. In other words UBL and UBH panels as well as UGL and UGH panels yielded fatigue lives which are almost similar for practical view point. It can be concluded therefore that the tension steel does not significantly improve the fatigue life in punching failure, although it should be recognized that punching capacity increases with increasing amount of tension steel. Thus, for identical fatigue life in punching, the panels with higher tension steel must be subjected to higher maximum load level than the panels with lower amount of steel.

An attempt has been made to express the theoretical fatigue life N by considering a linear relationship between P/Pu and Log N for the limited test data. Figs. 4.16 and 4.17 show the proposed linear relationships which are identical and are of the form:

$$P/Pu = 1.0-0.0673\ \text{Log}N \quad N<2\times10^{6} \qquad (4.2)$$

For restrained panels it was not possible to express the theoretical fatigue life as a linear relationship but a bi-linear relation was found to be more representative.

The fatigue data for all four types of panels, namely UBL, UBH, UGL and UGH, are shown collectively in Fig. 4.18 as a single plot of P/Pu versus Log N. Equation 4.2 is also shown in Fig. 4.18 to graphically demonstrate the reasonable correlation of the proposed fatigue life equation to the

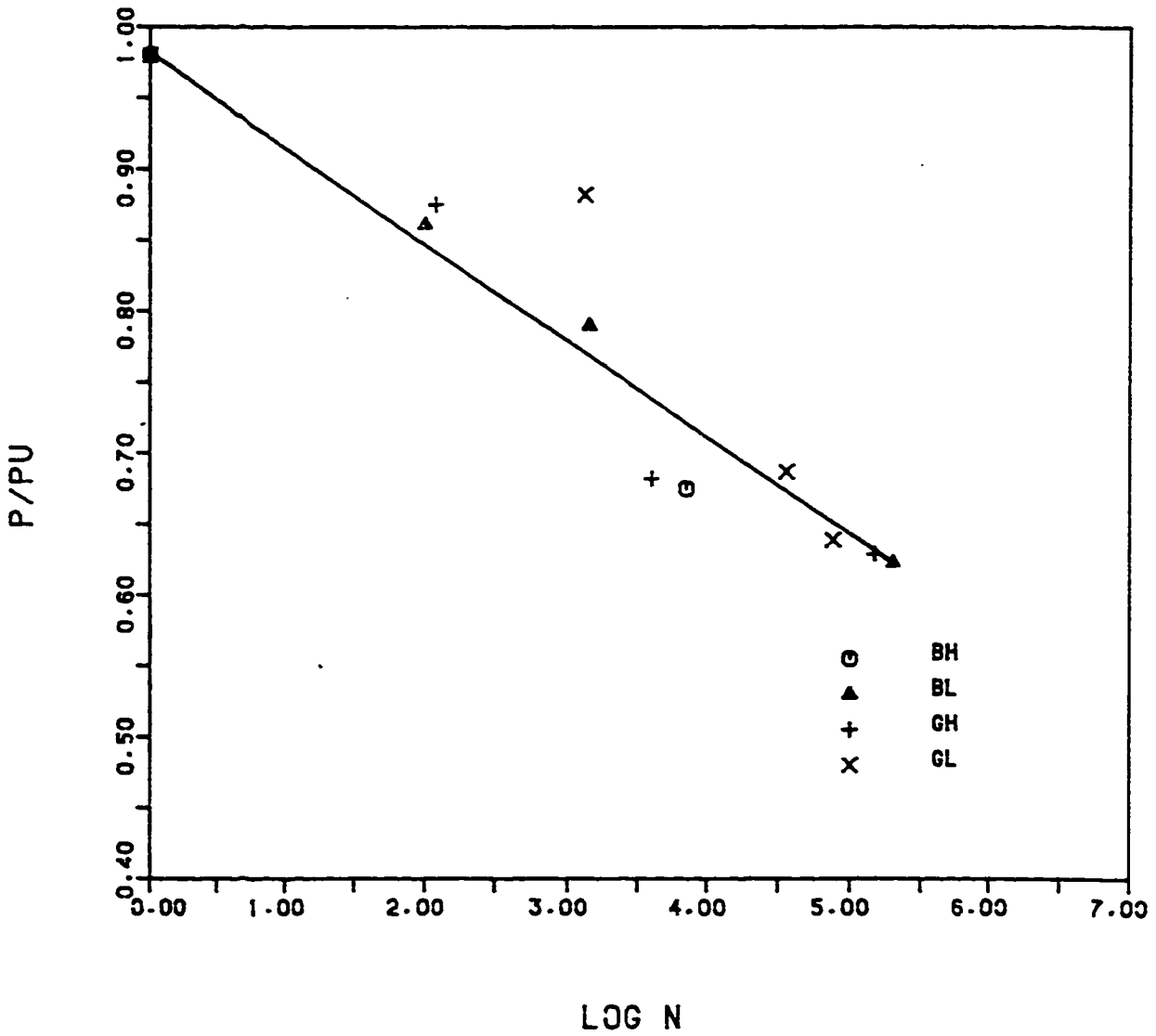

Fig. 4.18: S-N Diagram for Unrestrained Panels.

actual data. As seen from Fig. 4.18, the fatigue lives of panels UB and UG can be considered to be more or less similar without significant variation in log scale. A similar conclusion that was drawn for restrained panels can also be extended to unrestrained panels. The non-dimensionalized plots of P/Pu versus Log N in punching failure would not show any significant difference between the types of concrete for all practical purposes. The predicted fatigue life can be taken as independent of the type of concrete.

The fatigue failure pattern of unrestrained panels in punching is similar to that was noticed in static tests, (Plate 4.3). The failure zone encompasses a large area whose top corresponds to the loaded area and bottom covering almost the entire span. The failure is usually sudden but preceded by development of numerous cracks diverging from the central loaded area.

4.3 Effect of Edge Restraint

4.3.1 *Static Tests*

The theoretical ultimate punching loads for restrained panels which were computed in the previous chapter are listed along with the experimental results in Table 4.12 for the purpose of comparison. In all cases the theoretical

Table 4.12: Experimental versus Theoretical Punching Load for Restrained Panels.

Panel Type	Bearing Area	Theoretical/Punching Load (kN)		Experimental Failure Load (kN)
		Method 1	Method 2	
BL	50 x 100 mm	72	78	97
	100 x 200 mm	88	110	139
GL	50 x 100 mm	70	70	115
	100 x 200 mm	82	78	128
GH	50 x 100 mm	100	70	138
	100 x 200 mm	109	102	147

Method 1 using Kinnunen and Nylander Model

Method 2 using plasticity approach.

load obtained by any of the two methods, i.e. Kinnunen and Nylander model or plasticity approach, was less than the experimental value. One of the major causes of this lower theoretical values may be attributed to the favourable influence of support restraint, as edge restraint has been shown to increase the punching capacity of slabs (3). As the plasticity model does not take into account the effect of tension steel, for panels with high steel (GH steel) this method grossly underestimates the true punching load. In the absence of results with and without support restraint for identical slabs, it is difficult to quantify the magnitude of the support restraint's contribution. If the model of Kinnunnen and Nylander which takes into account steel reinforcement is accepted as a good theoretical approach, results of Table 4.4 would show that theoretical values are less than actual values. Part of this increase is solely due to the favourable influence of support restraint.

4.3.2 *Fatigue Tests*

To examine the effect of edge restraint on the fatigue life of slabs, Fig. 4.18 was constructed by superimposing the two S-N diagrams for restrained and unrestrained panels. As discussed earlier, both S-N diagrams can be taken as independent of steel and type of construction. The

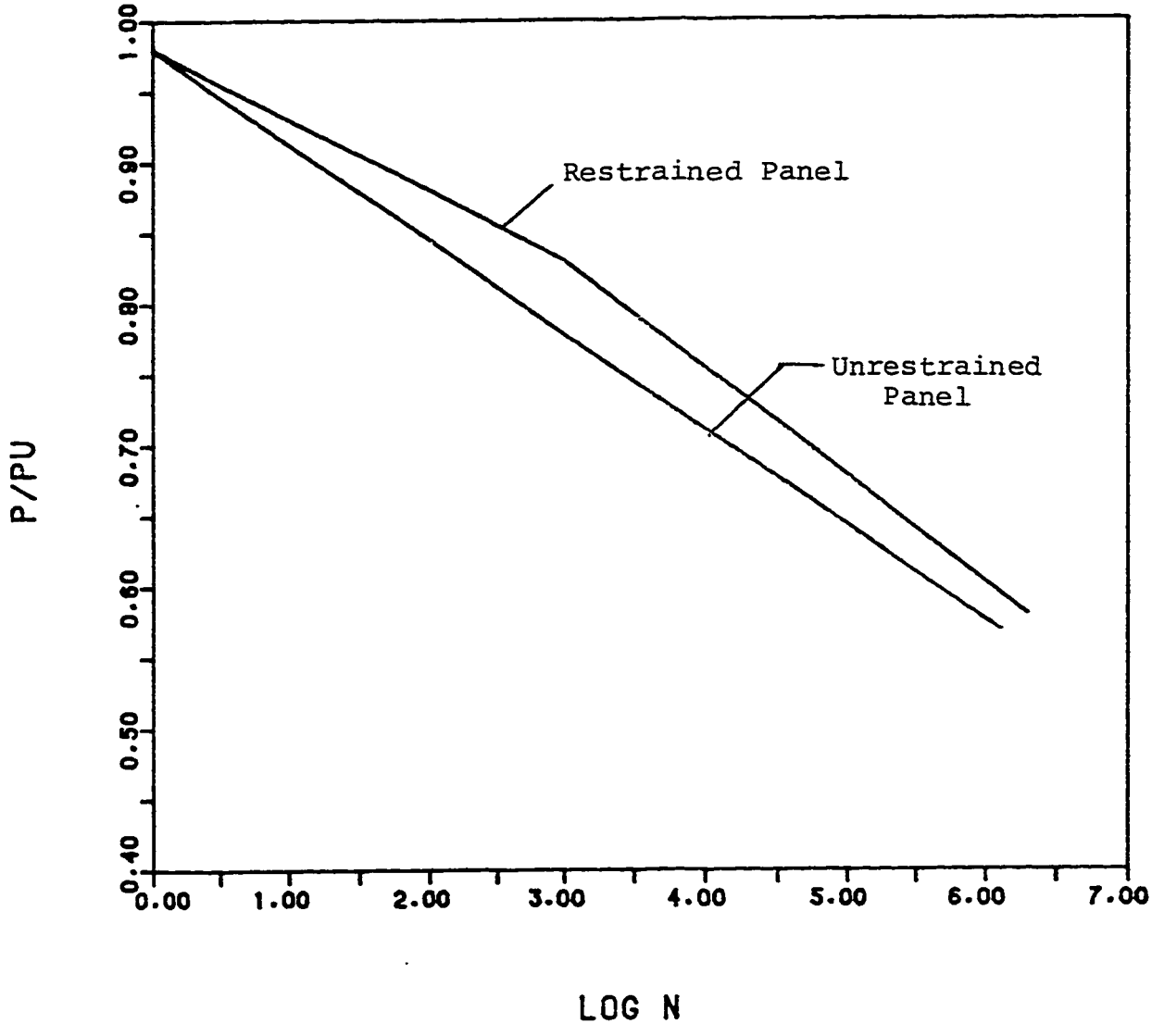

Fig. 4.19: S-N Diagram for Restrained and Unrestrained Panels.

difference between these two idealized plots (Fig.4.19) could partly be attributed to the effect of support restraint as this was the most significant difference between the two types of panels. As seen from Fig. 4.19 the fatigue life of restrained slabs in punching would be slightly higher than that of unrestrained panels under identical P/Pu values. Although the difference is not very significant, the consistent higher values of N (for the same P/Pu) for restrained panels indicates that the fatigue life is likely to be improved for restrained panels.

CHAPTER 5

SUMMARY AND CONCLUSIONS

5.1 Summary

An experimental study was undertaken on two types of reinforced concrete deck slabs to examine the static and fatigue failure of deck slabs. The two types of deck slabs considered in this study are: (i) large size simulated panels of girder-slab type bridge deck and (ii) small size panels. Static tests to evaluate the ultimate load carrying capacity were carried out on the restrained panels using two different areas of the patch load. Both the two patch load areas induced punching shear failure since the flexural capacity of the slab as calculated by the yield line theory, without taking the effect of edge restraint, was higher than the experimental punching load. On the small panels punching shear capacity was determined using one value for the loaded area. Based on the results of the static tests, fatigue tests were conducted using 0.9, o.8, 0.7 and 0.6 Pu as the maximum load of the fatigue cycle. The load ratio was kept about 0.1 for all fatigue tests.

Two significant aspects of this study were to observe the influence of initial non-structural precracks in deck

slabs which result from construction related causes such as plastic shrinkage and plastic settlement and to observe the influence of the edge restraint of the slab on the punching capacity and fatigue life.

5.2 Conclusions

Based on this study, the following conclusions can be drawn:

1) The punching capacity of the slab is impaired by the presence of non-structural precracks which reduce the punching load capacity. The punching capacity is enhanced to a certain degree by the increase in the main tension steel reinforcement.
2) The load-deflection response of the restrained slabs can be considered to be essentially linear upto about 70% of the ultimate punching load. The nonlinear effect due to in-plane membrance forces is not very pronounced at lower load level.
3) Fatigue life of a restrained deck slab can be approximated by a bi-linear relationship as proposed between nondimensionalized load parameter and the number of cycles to failure. This relationship is independent of the type of concrete, either good or bad construction, and the concrete strength. Support restraints tend to improve fatigue life of

deck slab by a small degree. Fatigue life for a loads level below 0.5 Pu is expected to exceed 2 million cycles.

4) Fatigue failure under a patch load is sudden and occurs with progressive nucleation of fracture cracks. The failure is characterized by fracture of a conical area of concrete whose top corresponds to the loaded area and bottom encompasses a relatively large area.
5) The punching load capacity calculated in accordance with the ACI Specification is considerably less than the failure load. Thus ACI predicted values are conservative and safe for design.
6) For restrained panels the mathematical models of Kinnunen and Nylander (7) and the plasticity approach (24) gave an analytical punching load which was always less than the experimental punching load. The increase in the capacity is believed to result from the edge restraint provided by the longitudinal beams and transverse diaphragms.

5.3 Future Recommendations

The present study concentrated on the behavior of reinforced concrete deck slabs under static and high level cyclic loads. However, further research is needed to

predict the fatigue life of reinforced concrete slabs at lower load levels to meaningfully determine the endurance limit for slabs in punching shear type failure.

The effect of edge restraint provided by edge beams and diaphragms on the punching shear capacity of reinforced concrete slabs was observed in this study but a quantitative value for the increase in punching capacity due to edge restraint was not formulated. Research in this direction can be carried out to determine influence of support restraints in girder-slab type bridges.

Finally new research should be directed towards the area of prediction of failure mode according to the geometry of the slab and patch load area under consideration. It would be of interest to define the relative size of the contact area above which no punching failure can take place and the capacity of the deck slab can be effectively utilized.

REFERENCES

1. Csagoly, P. F., "Design of Thin Concrete Deck Slabs by the Ontario Highway Bridge Design Code", Report No. SRR-79-11, Ministry of Transportation and Communications, Ontario, Canada, 1979.
2. Brian, E. Hewitt and Barrington de V. Bachelor, "Punching Shear Strength of Restrained Slabs", Journal of the Structural Division, ASCE, 101, (ST9), September 1975, pp. 1837-1853.
3. Taylor and Hayes, "Some Tests on the Effect of Edge Restraint on Punching Shear in Reinforced Concrete Slabs", Magazine of Concrete Research, Vol. 17, 1965, pp. 39-44.
4. Aoki, Y., and Seki, H., "Shearing Strength and Flexural Cracking and Capacity of Two-Way Slab Subjected to Concentrated Load", Cracking, Deflection and Ultimate Load of Concrete Slab Systems (SP-30), Detroit, ACI, 1971, pp. 103-126.
5. Bachelor and Tissington, "Shear Strength of Two-Way Bridge Slabs", Journal of the Structural Division, ASCE, Vol. 102. No. ST 12, December 1976, pp. 2315-2331.
6. Bachelor and Tong, "Compressive Membrane Enhancement in

Two-Way Bridge Slabs", Cracking, Deflection and Ultimate Load of Concrete Slab Systems (SP-30), Detriot, ACI, 1971, pp.271-286.

7. Kinnunen and Nylander, "Punching of Concrete Slabs Without Shear Reinforcement", Transactions of the Royal Institute of Technology, Stockholm, Sweden, No. 158, 1960.

8. Kinnunen, "Punching of Concrete Slabs with Two-Way Reinforcement", Transactions of the Royal Institute of Technology, Stockholm, Sweden, No. 198, 1963.

9. Brotche, J., and Halley, M., "Membrane Action in Slabs", Cracking, Deflection and Ultimate Load on Concrete Slab Systems (SP-30), Detroit, ACI, 1971, pp. 345-377.

10. The Shear Strength of Reinforced Concrete Members - Slabs", ASCE-ACI Committee 426, Journal of the Structural Division, ASCE, Vol.100, No.STB, Proc. Paper 10733, August 1974, pp. 1543-1591.

11. Nordby, "Fatigue of Concrete - A Review of Research", Proceedings of the American Concrete Institute, Vol. 55, August 1958, pp. 191-215.

12. Ralejs Topfers and Thomas Kutli, "Fatigue Strength of Plain, Ordinary and Lightweight Concrete", Journal of the American Institute, Vol. 76, No. 5, May 1979.

13. Abeles, "Static and Fatigue Tests on Partially

Prestressed Concrete Constructions", Journal of the American Concrete Institute, December 1954.

14. ACI Committee 215, Abeles Symposium, "Fatigue of Concrete", ACI, SP-41, Detroit, 1974.
15. ACI Committee 215, "Considerations for Design of Concrete Structures Subjected to Fatigue Loading". Journal of the American Concrete Institute, Vol. 71, No.3, March 1974.
16. ACI Committee 215, (Editors: Shah, S. P.), "Fatigue of Concrete Structures", ACI, SP-75. Detroit, 1982, 401 pp.
17. Chang and Kesler, "Static and Fatigue Strength in Shear of Beams with Tensile Reinforcement", Journal of the American Concrete Institute, June 1958.
18. Chang and Kesler, "Fatigue Behavior of Reinforced Concrete Beams", Journal of the American Concrete Institute, August 1958.
19. Week, "The Fatigue Strength of Reinforcing Bars in Concrete Beams", Nordic Concrete Research, No. 1, December 1982.
20. B. dev. Bachelor and B., E. Hewitt, "Are Composite Bridge Slabs Too Conservatively Designed - Fatigue Studies", Fatigue of Concrete (SP-41) Detroit, ACI, 1974, pp. 331-346.
21. Okada, Okamura and Sonoda, Transportation Research

Record No.664. "Bridge Engineering", Vol. 1, Proceeding of a conference conducted by the Transportation Research Board, September 25-27, 1978.

22. Okada, Okamura and Sonoda, "Cracking and Fatigue Behavior of Bridge Deck RC Slabs", Transaction of JSCE, Vol. 14, 1982.

23. Park and Gamble, "Reinforced Concrete Slabs", John Wiley and Sons, New York, 1980.

24. M. P. Neilsen, "Limit Analysis and Concrete Plasticity", in, Prentice-Hall, Inc., Englewood Cliffs, New Jersey 1984.

25. "Building Code Requirements for Reinforced Concrete", ACI 318-83, Detroit, 1983.

26. A. Ingerslev, "The Strength of Rectangular Slabs", J. Inst., Struct. Eng., Vol. 1, No.1, January 1923., 1974, pp. 677-720.

27. Johansen, "Yield Line Theory" translated by Cement and Concrete Association, London, 1962.

28. Eyre, Riba and Kemp, "A Graphical Solution for Predicting the Increase in Strength of Concrete Slabs Due to Membrane Action", Magazine of Concrete Research, Vol. 35, No. 124, September 1983.

29. ACI Committee 215, "Fatigue of Concrete", ACI Bibliography No. 3, ACI, Detroit, 1960, 38 pp.

30. Ralejs Topfers, "Tensile Fatigue Strength of Plain

Concrete", Journal of the American Concrete Institute, Vol. 76, No. 8, August 1979.

31. Hawkins, Criswell and Roll, "Shear Strength of Slabs Without Shear Reinforcement", ACI, SP-42, Detroit, 1974, pp. 677-720.

32. Hawkins and Criswell, "Shear Strength of Slabs; Basic Principles and Their Relation to Current Methods of Analysis", ACI, SP-42, Detroit, 1974, pp.641-676.

33. Abul K. Azad, MASCE, Mohammed H. Baluch, Mustafa Al-Mandil and Mohammad Al-Sawaiyan, "Static and Fatigue Tests of Simulated Bridge Decks", Proceedings of the session on Experimental Assessment of Performance of Bridges, ASCE Annual Convention, Boston, Oct. 27-31, 1986, pp.30-41.

APPENDIX

Computer Program Listing

```
FILE: HEWITT2  WATFIV   A1  UNIVERSITY OF PETROLEUM & MINERALS, DHAHRAN

$JOB
C       THIS PROGRAM CALCULATES THE PUNCHING CAPACITY OF
C       SLABS WITH NO EDGE RESTRAINTS USING KINNUNEN AND
C                    NYLANDER MODEL
C       ***************************************************
C       THE FOLLOWING SYMBOLS ARE USED IN THIS PROGRAM
C       CP = DIAMETER OR EQUIVALENT DIAMETER OF LOADED AREA
C       D  = EFFECTIVE DEPTH OF SLAB
C       FCUBE = CONCRETE CUBE COMPRESSIVE STRENGTH
C       CS = DIAMETER OR EQUIVALENT DIAMETER OF SLAB
C       RAW= REINFORCEMENT RATIO
C       FY =YIELD STRESS OF REINFORCEMENT
C       ES =MODULUS OF ELASTICITY OF REINFORCING STEEL
C       X  = 0.0 INDEX FOR SIMPLE SLABS
C       ***************************************************
C       THIS PROGRAM USES THE FOLLOWING UNITS
C         LENGTH    CENTIMETERS
C         STRESS     KGF/CM**2
C       ***************************************************
C
        READ,CP,D,FCUBE,CS,RAW,FY,ES,X
        DO 90 I=39,60
        Y=I*D/100.
        CALL SUBFT(FCUBE,CP,D,FT)
        CALL SOLVER(Y,CP,CS,D,X,ALFA1,KZ)
        CALL CALCU(CP,D,Y,FCUBE,ALFA1,P2,FT)
        CALL SUBPSI(CP,D,Y,PSI)
        RS=ES*PSI*(D-Y)/FY
        CO=0.5*CP+1.3*D
        IF(RS.LT.CO)GO TO 60
        R1=RAW*FY*D*((RS-CO)+RS*ALOG(CS/(2.*RS)))
        R2B=RAW*FY*D*CO
        GO TO 70
60      R1=RAW*FY*D*RS*ALOG(CS/(2.*CO))
        R2B=RAW*FY*D*RS
70      P1=(2.*3.14/KZ)*(R1+R2B)
        ERRR=(P2-P1)/P2
        ERROR=ABS(ERRR)*100.
        IF(ERROR.LE.5.0)THEN
        P=P1
        Y1=Y
        ERR=ERROR
        END IF
90      CONTINUE
445     PRINT,'ERROR',ERR
        P=1.2*4.443*P/454.
        IF(ERR.LT.5.0)PRINT,'ULTIMATE CAP',P
        STOP
        END
C       ***************************************************
        SUBROUTINE SUBPSI(CP,D,Y,PSI)
        E=CP/D
        IF(E.GT.2.)GO TO 20
        PSI=0.0035*(1.-0.22*(CP/D))*(1.+(CP/Y))
        GO TO 40
```

```
20      PSI=0.0019*(1.+(CP/(2.*Y)))
40      RETURN
        END
C       ***********************************************************************
        SUBROUTINE CALCU(CP,D,Y,FCUBE,ALFA,P,FT)
        A=3.14*FT*CP*Y*(CP+2.*Y)/(CP+Y)
        FALFA=TAN(ALFA)*(1.-TAN(ALFA))/(1.+(TAN(ALFA)**2))
        P=A*FALFA
        RETURN
        END
C       ***********************************************************************
        SUBROUTINE SUBFT(FCUBE,CP,D,FT)
        E=CP/D
        IF(E.GE.2.0)GO TO 40
        FT=825.*(0.35+0.3*(FCUBE/150.))*(1.-0.22*(CP/D))
        GO TO 30
40      FT=400.*(0.35+0.3*(FCUBE/150.))
30      RETURN
        END
C       ***********************************************************************
        SUBROUTINE SOLVER(Y,CP,CS,D,X,ALFA1,KZ)
        DO 60 I=1,360
        II=I-1
        ALFA=3.14*II/180.
        A=(1.-TAN(ALFA))/(1.+(TAN(ALFA))**2)
        KZ=(3.*(CS-CP)/(2.*(3.*D-Y)))-(3.*X*CS/(4.*(3.*D-Y)))
        R=((KZ*TAN(ALFA))-1.)*A
        R2=(1.+Y/CP)*ALOG(CS/(CP+2.*Y))
        R2=R2/4.7
        ER=(R2-R)/R
        ERR=ABS(ER)*100.
        IF(ERR.LT.5.0)THEN
        ALFA1=ALFA
        END IF
60      CONTINUE
        RETURN
        END
$ENTRY
16.3 8.2 187.    95. 0.0092 3515. 2039000.  0.
```

340